3

Steady axisymmetric and related flows

3.1 Circular pipe flow

We begin this chapter with a discussion of the flow within a circular pipe, including the flow in the annulus between concentric circular pipes. With the flow driven along the pipe by a uniform pressure gradient we have the analogue of plane Poiseuille flow. In the absence of any pressure gradient a flow may be induced by the motion of one cylinder relative to another, either by a sliding motion parallel to the cylinder generators or by relative rotation about their common axis, which may be considered the analogue of plane Couette flow.

If the velocity components are assumed to be independent of θ and z, that is $v_r = v_r(r)$, $v_\theta = v_\theta(r)$ and $v_z = v_z(r)$, the continuity equation (1.22) shows that

$$v_r = \frac{m}{r}. \tag{3.1}$$

The momentum equations (1.19) to (1.21) then simplify to

$$v_r \frac{\partial v_r}{\partial r} - \frac{v_\theta^2}{r} = -\frac{1}{\rho}\frac{\partial p}{\partial r}, \tag{3.2}$$

$$v_r \frac{\partial v_\theta}{\partial r} + \frac{v_r v_\theta}{r} = \nu\left(\frac{\partial^2 v_\theta}{\partial r^2} + \frac{1}{r}\frac{\partial v_\theta}{\partial r} - \frac{v_\theta}{r^2}\right), \tag{3.3}$$

$$v_r \frac{\partial v_z}{\partial r} = -\frac{1}{\rho}\frac{\partial p}{\partial z} + \nu\left(\frac{\partial^2 v_z}{\partial r^2} + \frac{1}{r}\frac{\partial v_z}{\partial r}\right), \tag{3.4}$$

where v_r is given by (3.1). Under the assumptions made, the case $m \neq 0$ is only possible if the cylinder boundaries, at $r = a, b$ $(b < a)$ are porous and the normal velocities there prescribed as m/a, m/b.

For the flows anticipated above, other boundary conditions to be applied are

$$v_\theta = a\Omega_a \quad \text{at} \quad r = a, \quad v_\theta = b\Omega_b \quad \text{at} \quad r = b, \tag{3.5}$$

and

$$v_z = 0 \quad \text{at} \quad r = a, \qquad v_z = W \quad \text{at} \quad r = b. \tag{3.6}$$

With the pressure field given as $p = -Pz + \tilde{P}(r)$, where P is a constant, equations (3.2) to (3.4), subject to (3.5), (3.6) may readily be solved for v_θ, v_z and $\tilde{P}$. However for convenience, and historical reasons, the cases of axial motion and circular motion are treated separately.

(i) Case $m = \Omega_a = \Omega_b = 0$ For this case both v_r, v_θ vanish, and the solution of equation (3.4), subject to (3.6), is

$$v_z = \frac{P}{4\mu}(a^2 - r^2) + \left\{ W + \frac{P}{4\mu}(b^2 - a^2) \right\} \frac{\ln(r/a)}{\ln(b/a)} \tag{3.7}$$

with the corresponding volume flux along the annulus given by

$$Q = \frac{\pi P}{8\mu} \left\{ a^4 - b^4 + \frac{(a^2 - b^2)^2}{\ln(b/a)} - \frac{8\mu W b^2}{P} - \frac{4\mu W}{P \ln(b/a)}(a^2 - b^2) \right\}. \tag{3.8}$$

The particular case with $W = 0$, when the flow is driven along the pipe by the pressure gradient alone, was first considered by Boussinesq (1868). The special case of (3.7), (3.8)

$$W = \frac{P b^2 \ln(b/a)}{2\mu} + \frac{P}{4\mu}(a^2 - b^2),$$

with

$$v_z = \frac{P}{4\mu}(a^2 - r^2) + \frac{P b^2}{2\mu} \ln(r/a) \tag{3.9}$$

and

$$Q = \frac{\pi P}{8\mu} \left\{ a^4 - b^4 + 4b^4 \ln(a/b) - 4b^2(a^2 - b^2) \right\} \tag{3.10}$$

has $\partial v_z / \partial r = 0$ at $r = b$. As a consequence it is possible, in equations (3.9) and (3.10), to allow $b \to 0$ and recover the classical solution for flow down a pipe of radius a under the action of a constant pressure gradient,

$$v_z = \frac{P}{4\mu}(a^2 - r^2), \quad \text{with} \quad Q = \frac{\pi P a^4}{8\mu}.$$

This famous result for the flux was first found empirically by Hagen (1839) and Poiseuille (1840), who independently measured the flow of water along capillary tubes. Stokes (1845) first solved the equations of motion to find (essentially) these results for pipe flow, in agreement with the measurements of Hagen and Poiseuille.

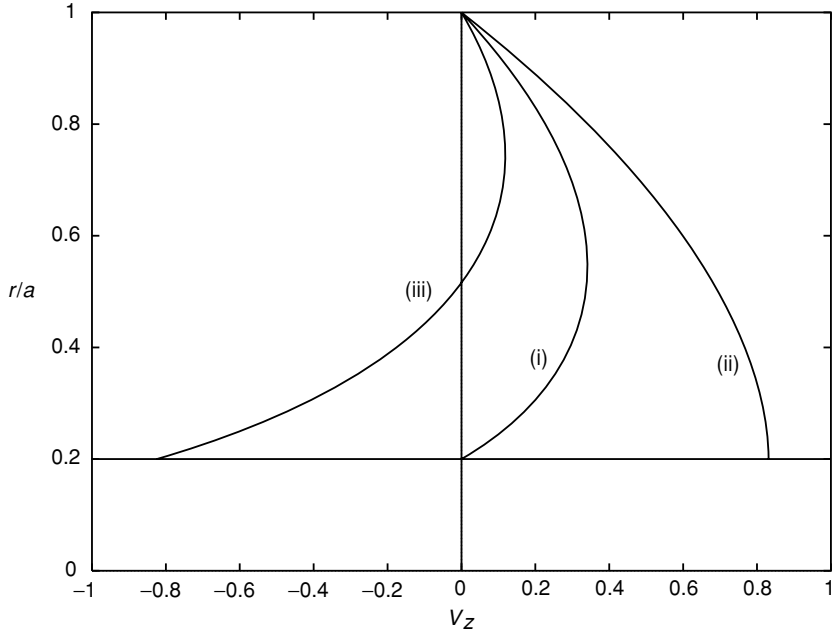

Figure 3.1 Annular pipe flow with non-zero axial pressure gradient P and $b/a = 0.2$. (i) The case $W = 0$, (ii) $W > 0$ with v_z as in equation (3.9), (iii) $W < 0$ such that $Q \equiv 0$.

The special case

$$\frac{P}{8\mu} = W\left[\frac{2b^2\ln(b/a) + a^2 - b^2}{2(a^2-b^2)\{(a^2+b^2)\ln(b/a) + a^2 - b^2\}}\right]$$

ensures $Q \equiv 0$. This finds application when the outer cylinder is of finite length L, and sealed at each end with the inner cylinder drawn through the seals, first discussed by Bouasse (see Berker (1963)). If $L \gg a$ the fully developed flow, (3.7), may be expected to be appropriate away from the ends.

Representative velocity profiles associated with these pipe flows are shown in figure 3.1.

(ii) Case $P = 0$ For this case, provided also $W = 0$, the flow may be driven by the rotation of the cylindrical boundaries which, for $m = 0$, may be expected to result in concentric circular streamlines or, if $m \neq 0$ corresponding to a source-like flow within the porous inner cylinder, spiral streamlines. The solution of equation (3.3) with conditions (3.5) is, with $v_r = m/r$,

$$v_\theta = \frac{a^2b^2(a^R\Omega_b - b^R\Omega_a)}{a^{R+2} - b^{R+2}}\frac{1}{r} + \frac{a^2\Omega_a - b^2\Omega_b}{a^{R+2} - b^{R+2}}r^{R+1} \tag{3.11}$$

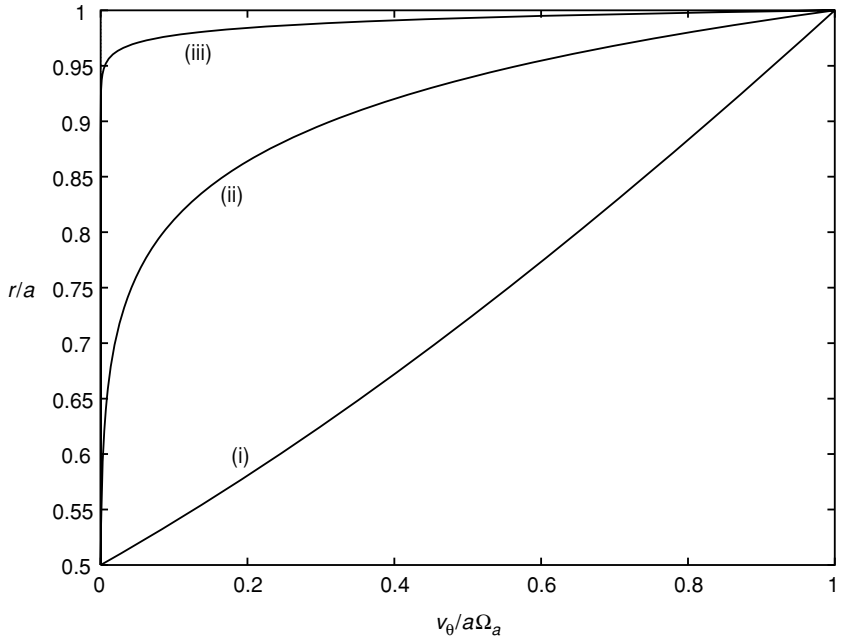

Figure 3.2 Annular pipe flow with $P = W \equiv 0$ and $b/a = 0.5$. The case $\Omega_b = 0$ is illustrated with (i) $R = 0$, (ii) $R = 10$, (iii) $R = 100$. As R increases the boundary-layer nature of the flow is apparent.

where $R = m/\nu$ is a Reynolds number or, in the exceptional case $R = -2$

$$v_\theta = \frac{b^2\Omega_b \ln a - a^2\Omega_a \ln b}{\ln(a/b)} \frac{1}{r} + \frac{a^2\Omega_a - b^2\Omega_b}{\ln(a/b)} \frac{\ln r}{r}.$$

The pressure function $\tilde{P}(r)$ follows from equation (3.2). These solutions were obtained by Hocking (1963), who commented on the case of high Reynolds number, $R \gg 1$, for which, from (3.11)

$$v_\theta \simeq \frac{b^2\Omega_b}{r} + \{a\Omega_a - (b^2/a)\Omega_b\} \left(\frac{r}{a}\right)^{R+1}.$$

It is clear that in this case, with the second term negligible unless $r \approx a$, the azimuthal velocity behaves as a potential vortex. In other words fluid particles issuing from the inner cylinder retain their initial angular momentum until the viscous torque close to $r = a$ changes it. As a consequence the flow divides into an essentially inviscid potential core with a thin boundary layer close to $r = a$, whose thickness may be estimated as $O(aR^{-1})$. Profiles of the velocity

component v_θ for various values of R in the special case $\Omega_b = 0$ are shown in figure 3.2.

For $R = 0$, corresponding to impermeable boundaries, the only non-zero component of velocity is v_θ given, from equation (3.11), as

$$v_\theta = \frac{a^2 b^2 (\Omega_b - \Omega_a)}{a^2 - b^2} \frac{1}{r} + \frac{a^2 \Omega_a - b^2 \Omega_b}{a^2 - b^2} r,$$

a solution whose form was known to Stokes (1845). For this case the moment per unit length of each fluid cylinder of radius r is

$$M = -4\pi \mu a^2 b^2 \left(\frac{\Omega_a - \Omega_b}{b^2 - a^2} \right).$$

Viscometers based upon Poiseuille flow or concentric rotating cylinders have been used for determining the viscosity of fluids, Mallock (1896).

A steady flow external to the cylinders can, in general, only be sustained if suction is applied at the cylinder. Consider a uniform axial flow $(0, 0, W)$ external to the porous cylinder $r = a$. Stuart (1966b) has shown that the appropriate solution is

$$v_r = -\frac{m}{r}, \quad v_z = W \left\{ 1 - \left(\frac{a}{r} \right)^R \right\}, \quad R = \frac{m}{\nu},$$

noting that for $R \gg 1$ a boundary layer forms at $r = a$. For the flow external to a circular cylinder radius a, rotating with angular velocity Ω_a, a steady solution is only available if the circulation at large distances, Γ, is the same as at the cylinder so that $\Gamma = 2\pi a^2 \Omega_a$ with $v_\theta = a^2 \Omega_a / r$. Otherwise, as noted by Preston (1950), suction is required to maintain a steady flow with, again, $v_r = -m/r$ and

$$v_\theta = \frac{\Gamma}{2\pi r} + \left(a\Omega_a - \frac{\Gamma}{2\pi a} \right) \left(\frac{a}{r} \right)^{R-1}, \quad R \neq 2,$$

$$v_\theta = \frac{\Gamma}{2\pi r} + \left(a\Omega_a - \frac{\Gamma}{2\pi a} \right) \frac{a}{r} \frac{\ln r}{\ln a}, \quad R = 2.$$

Accordingly, even when suction is applied, for $R \leq 2$ the only steady flow with finite circulation at infinity has $\Gamma = 2\pi a^2 \Omega_a$. But if the suction velocity exceeds $2\nu/a$ different values of the circulation may be maintained at infinity and the cylinder.

Berman (1958a) has considered axial flow driven by a constant pressure gradient along the annulus for $m \neq 0$ in the absence of rotation.

3.2 Non-circular pipe flow

For flow driven along a pipe of elliptic section, say $x^2/a^2 + y^2/b^2 = 1$, with a constant pressure gradient $-P$, Boussinesq (1868) found that

$$w(x, y) = \frac{Pa^2b^2}{2\mu(a^2 + b^2)}\left(1 - \frac{x^2}{a^2} - \frac{y^2}{b^2}\right),$$

with

$$Q = \frac{\pi P a^3 b^3}{4\mu(a^2 + b^2)}.$$

The eccentricity of the ellipse is $e = (1 - b^2/a^2)^{1/2}$ where a is the semi-major axis. The flow becomes Poiseuille flow in a circular pipe when $e = 0$, so that $a = b$, and plane Poiseuille flow in a channel as $a \to \infty$ with b fixed.

A wide variety of pipes with other cross-sections have been considered. For example, a sector of a circle with boundaries $r = 0, a$, $\theta = \pm\alpha$; a curvilinear rectangle bounded by two concentric circular arcs $r = a, b$ and two radii; the annulus bounded by two eccentric circles or two confocal ellipses; a lemniscate; a circle 'notched' by an arc of another circle; a limaçon; a cardioid. Berker (1963) gives a comprehensive bibliography and discusses some of these in detail.

3.3 Beltrami flows and their generalisation

As already noted in section 2.2, steady Beltrami flows for which $\mathbf{v} \wedge \boldsymbol{\omega} = \mathbf{0}$ can only exist in a viscous fluid when sustained by a non-conservative body force. The generalised Beltrami flows are required to satisfy equations (2.14) and (2.15). For axisymmetric flows we have $\mathbf{v} = (v_r, 0, v_z)$ and $\boldsymbol{\omega} = (0, \omega_\theta, 0)$. With $\boldsymbol{\omega} = \nabla \wedge \mathbf{v}$, and introducing the stream function ψ as in equation (1.24), we have

$$\frac{\partial}{\partial r}\left(\frac{1}{r}\frac{\partial \psi}{\partial r}\right) + \frac{1}{r}\frac{\partial^2 \psi}{\partial z^2} = -\omega_\theta, \tag{3.12}$$

whilst equations (2.14) and (2.15) require

$$\frac{\partial}{\partial r}\left(\frac{\omega_\theta}{r}\frac{\partial \psi}{\partial z}\right) - \frac{\partial}{\partial z}\left(\frac{\omega_\theta}{r}\frac{\partial \psi}{\partial r}\right) = 0, \tag{3.13}$$

and

$$\frac{\partial}{\partial r}\left\{\frac{1}{r}\frac{\partial (r\omega_\theta)}{\partial r}\right\} + \frac{\partial^2 \omega_\theta}{\partial z^2} = 0. \tag{3.14}$$

Now, equation (3.13) has the solution $\omega_\theta = rf(\psi)$ showing that ω_θ/r is a constant along streamlines. However, Marris and Aswani (1977) have determined that the only possibility for these axisymmetric generalised Beltrami flows is that $f =$ constant, or $\omega_\theta = \alpha r$. That being so, equation (3.14) is satisfied identically, and the remaining equation (3.12) to be solved for ψ is

$$\frac{\partial^2\psi}{\partial r^2} - \frac{1}{r}\frac{\partial\psi}{\partial r} + \frac{\partial^2\psi}{\partial z^2} = -\alpha r^2. \tag{3.15}$$

A simple, but useful, set of solutions of equation (3.15) is

$$\psi = c_1 r^4 + c_2 r^2 z^2 + c_3 r^2 + c_4 r^2 z + c_5(r^6 - 12r^4 z^2 + 8r^2 z^4),$$

where $8c_1 + 2c_2 = -\alpha$, but the c_i are otherwise arbitrary. For various combinations consider the following.

(i) $c_1, c_4 \neq 0$. Without loss of generality we may take $\psi = ar^2(br^2 - z)$, Berker (1963), which corresponds to two opposing rotational streams divided by the paraboloidal stream surface $z = br^2$.

(ii) $c_2 \neq 0$. The solution $\psi = c_2 r^2 z^2$ is a special case of solutions obtained by Agrawal (1957), discussed in more detail in section 3.7. This particular solution may be interpreted as rotational flow against the plane boundary $z = 0$ at which the no-slip condition is satisfied.

(iii) $c_1, c_2, c_3 \neq 0$. Again without loss of generality, the solution may be taken as

$$\psi = ar^2\left(\frac{r^2}{b^2} + \frac{z^2}{c^2} - 1\right).$$

With $b \neq c$ this represents the ellipsoidal vortex of O'Brien (1961), whilst with $b = c$ we have Hill's (1894) spherical vortex with radius b. In the latter case the spherical vortex may be immersed in a stream, uniform at infinity, with the velocities, but not the stresses, continuous across the spherical interface, see Acheson (1990).

(iv) $c_1, c_3, c_5 \neq 0$.

In this case the solution, discovered by Wang (1990a), may be written as

$$\psi = r^2\{ar^2 + b + c(r^4 - 12r^2 z^2 + 8z^4)\}. \tag{3.16}$$

Solutions not dissimilar to Hill's spherical vortex, in the sense of a toroidal vortex bounded by a closed stream surface, can be constructed from (3.16). An example is given in figure 3.3 where a relatively elongated toroidal vortex is shown.

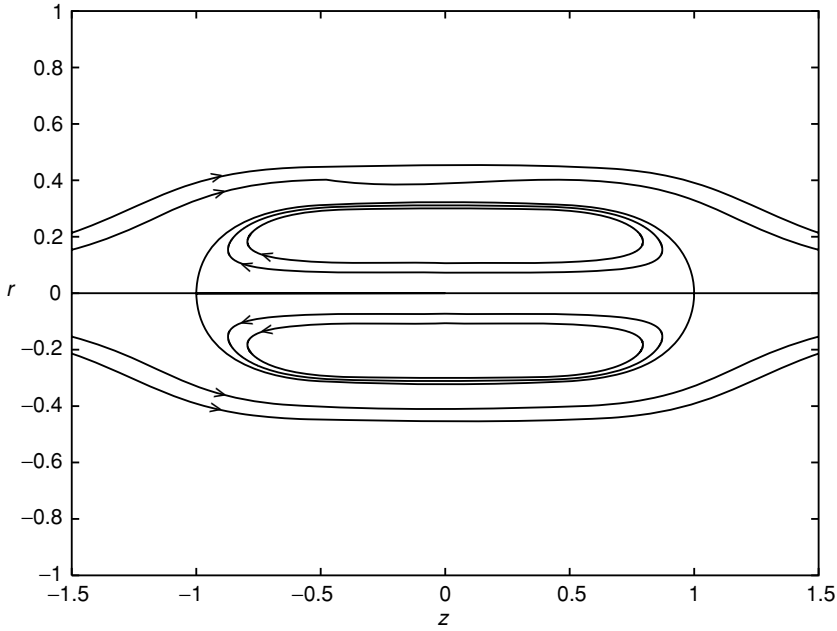

Figure 3.3 Wang's toroidal vortex, equation (3.16) with $a = 10$, $b = -1$, $c = \frac{1}{8}$. Commencing with the innermost the streamsurfaces have $\psi = -0.005$, $-0.01, 0, 0.1, 0.2$.

Additional solutions of the homogeneous form of equation (3.15) have been obtained by Berker (1963) as

$$\psi = r\left\{A_k J_1(kr) + B_k Y_1(kr)\right\}\left(C_k\,\mathrm{e}^{kz} + D_k\,\mathrm{e}^{-kz}\right)$$

where J_1, Y_1 are Bessel functions of the first and second kinds respectively.

As a utilisation of this consider the flow represented by

$$\psi = \frac{Pa^4}{16\mu}\left\{2\left(\frac{r}{a}\right)^2 - \left(\frac{r}{a}\right)^4\right\} + \sum_{k=1}^{\infty} c_k \left(\frac{r}{a}\right) J_1(\lambda_k r/a)\,\mathrm{e}^{\lambda_k z/a}. \tag{3.17}$$

The first term of equation (3.17) may be recognised as the Poiseuille pipe flow considered in section 3.1, the second term, a distortion of this, will satisfy the no-slip condition at $r = a$ provided that the constants λ_k are the zeros of the Bessel function J_0. At $r = a$ the normal component of velocity is then given by

$$v_r|_{r=a} = \frac{1}{a^2}\sum_{k=1}^{\infty} c_k J_1(\lambda_k)\,\mathrm{e}^{\lambda_k z/a}. \tag{3.18}$$

The solution (3.17) was introduced by Terrill (1982) who discusses various situations in which (3.18) represents the transpiration velocity across the porous pipe $r = a$.

Additional solutions which include the effects of swirl in generalised Beltrami flows have been discussed by Weinbaum and O'Brien (1967).

3.4 Stagnation-point flows

3.4.1 The classical Homann (1936) solution

In section 2.3 we discussed the flow in the immediate vicinity of the stagnation line on a rigid stationary cylinder. The axisymmetric analogue of that arises, for example, at the front stagnation point of a sphere placed in a uniform stream. Homann (1936) modelled this by the flow towards an infinite, rigid, stationary flat plate. This is, of course, a special case of the three-dimensional stagnation-point flow of section 2.5.4, but we include it here for completeness. In our formulation we allow the plate to slide in its own plane with constant velocity, and also allow for transpiration across it when porous; both of these features have been examined by Libby (1974, 1976) in the more general context of a three-dimensional stagnation point, whilst Wang (1973) has considered axisymmetric flow against a sliding plane.

The boundary is taken as $z = 0$, and with no natural length scale in the problem a self-similar solution with velocity components

$$v_r = krf'(\eta) + u_w \cos\theta g(\eta), \quad v_\theta = -u_w \sin\theta g(\eta),$$
$$v_z = -2(k\nu)^{1/2} f(\eta), \quad \eta = \left(\frac{k}{\nu}\right)^{1/2} z, \tag{3.19}$$

and pressure

$$\frac{p - p_0}{\rho} = -\frac{1}{2}k^2 r^2 - 2k\nu(f^2 + f'), \tag{3.20}$$

leads, using equations (1.19), (1.20), to the following equations for f and g,

$$f''' + 2ff'' - f'^2 + 1 = 0,$$
$$g'' + 2fg' - f'g = 0,$$

with boundary conditions

$$f(0) = \lambda, \quad f'(0) = 0, \quad f'(\infty) = 1, \quad g(0) = 1, \quad g(\infty) = 0.$$

With $\lambda = u_w = 0$ we recover the classical stagnation-point flow of Homann (1936). With $u_w \neq 0$ we have, without any loss of generality, the boundary

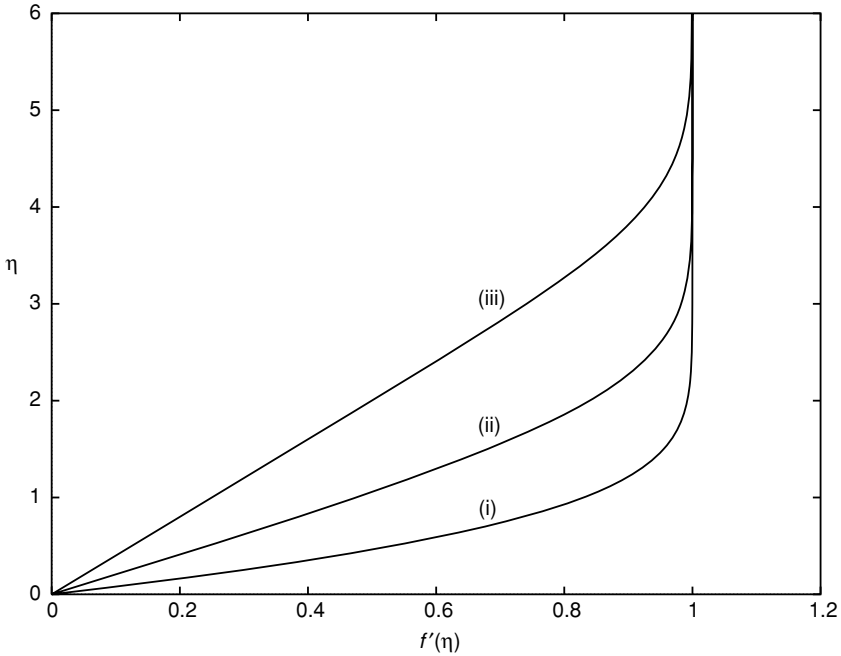

Figure 3.4 The radial velocity function $f'(\eta)$ at a stagnation point. (i) The case $\lambda = 0$ corresponds to the classical Homann flow, (ii) $\lambda = -1$, (iii) $\lambda = -2$.

sliding in its own plane with constant speed in the direction $\theta = 0$; this corresponds to the case addressed by Libby (1974) at a three-dimensional stagnation point, and by Wang (1973). For $\lambda \neq 0$ the boundary is assumed to be porous with transpiration across it, again a case considered by Libby (1976) (in fact, for a compressible fluid) at a three-dimensional stagnation point. For $\lambda < 0$ we have injection, perhaps the more interesting case, and in figure 3.4 we show profiles $f'(\eta)$ for various values of λ. As the injection rate increases the position η_0, where $f(\eta_0) = 0$, increases, with viscous effects increasingly unimportant for $\eta < \eta_0$. Corresponding profiles $g(\eta)$ are shown in figure 3.5. For $\eta < \eta_0$ there is again, relatively speaking, a lack of structure in the solution with a fairly rapid change taking place in the neighbourhood of $\eta = \eta_0$.

Davey (1963) has considered the solution at a three-dimensional stagnation point when the oncoming flow is rotational, and when the boundary itself may rotate. Here we present only the axisymmetric stagnation point, at a stationary

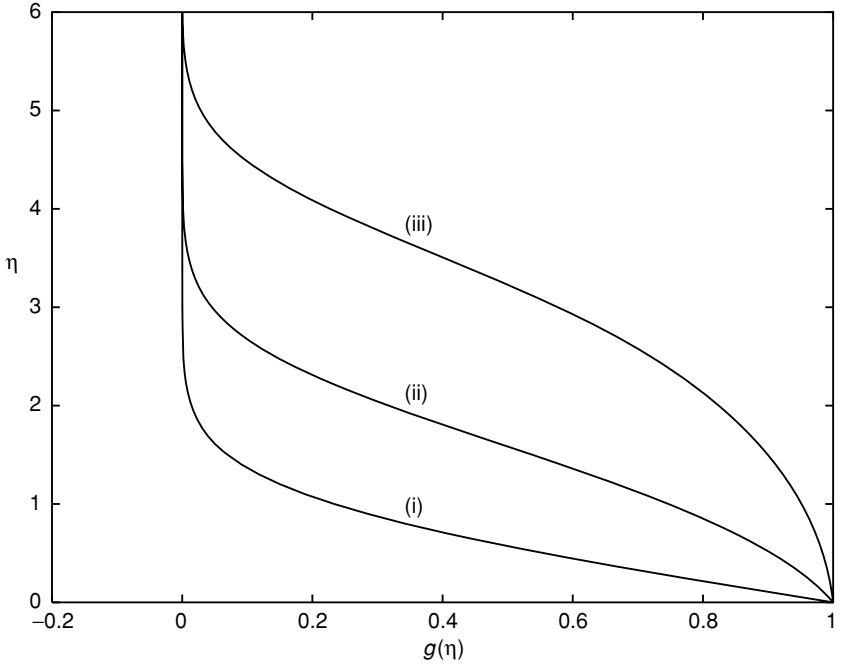

Figure 3.5 The velocity function $g(\eta)$ corresponding to boundary translation with speed u_w; see equation (3.19). (i) $\lambda = 0$, (ii) $\lambda = -1$, (iii) $\lambda = -2$.

plane boundary, with $\boldsymbol{\omega} = 2\Omega\mathbf{k}$ in the oncoming flow. Equations (3.19), (3.20) are replaced by

$$v_r = krf'(\eta),\ v_\theta = \Omega r g(\eta),\ v_z = -2(k\nu)^{1/2} f(\eta),\ \text{with again } \eta = \left(\frac{k}{\nu}\right)^{1/2} z,$$

and

$$\frac{p - p_0}{\rho} = \frac{1}{2}k^2r^2\left\{\left(\frac{\Omega}{k}\right)^2 - 1\right\} - 2\nu k(f' + f^2);$$

in addition a non-conservative body force is required to sustain this motion with $\mathbf{F} = 2\Omega kr\hat{\boldsymbol{\theta}}$. Ordinary differential equations for f and g are again derived from equations (1.19) and (1.20) as

$$f''' + 2ff'' - f'^2 + (\Omega/k)^2 g^2 + 1 - (\Omega/k)^2 = 0, \tag{3.21}$$

$$g'' + 2fg' - 2f'g + 2 = 0, \tag{3.22}$$

with boundary conditions

$$f(0) = f'(0) = g(0) = 0, \quad f'(\infty) = 1, \quad g(\infty) = 1. \tag{3.23}$$

Solutions of equations (3.21), (3.22) subject to (3.23) are shown in figure 3.6.

A practical application of the stagnation-point solution has been identified by Hinch and Lemaître (1994) to the problem of disks floating above an air table through which air is blown. Suppose two infinite planes are at a distance h apart. The upper is impermeable, the lower porous through which fluid is injected normally with uniform speed W. Then, if equations (3.19), (3.20) are replaced by

$$v_r = -\frac{Wr}{2h} f'(\eta), \quad v_z = Wf(\eta),$$
$$\frac{p - p_0}{\rho} = -\frac{1}{2}\frac{W^2}{h^2} r^2 \beta + \frac{W\nu}{h}\left(f' - \frac{1}{2}Rf^2\right),$$

where $\eta = z/h$, $R = Wh/\nu$, then equations (1.19) and (1.21) will be satisfied provided that

$$\frac{1}{R} f''' - ff'' + \frac{1}{2} f'^2 - 2\beta = 0, \tag{3.24}$$

which is to be solved subject to

$$f(0) = 1, \quad f'(0) = 0, \quad f(1) = f'(1) = 0.$$

Four boundary conditions for the third-order equation (3.24) reflect the fact that β is unknown *a priori*. Hinch and Lemaître present solutions across the whole range of Reynolds number R. Cox (2002) has extended the above to non-axisymmetric flow using the formulation of Howarth (1951) and Davey (1961). He concludes that for given W and h the non-axisymmetric flow, if achievable, can support a greater weight than the axisymmetric flow.

3.4.2 Stagnation on a circular cylinder

We have discussed the classical symmetric stagnation-point flows of Hiemenz (1911) and Homann (1936), and the asymmetric flows that link them detailed by Howarth (1951) and Davey (1961). A somewhat different stagnation flow was discovered by Wang (1974), namely that on a circle of radius a, circumscribing a circular cylinder of the same radius whose generators lie in the z-direction. For an inviscid fluid it is easily verified that this stagnation flow has

$$v_r = -k\left(r - \frac{a^2}{r}\right), \quad v_z = 2kz, \quad \frac{p - p_0}{\rho} = -2k^2 z^2 - \frac{1}{2}k^2\left(r - \frac{a^2}{r}\right)^2. \tag{3.25}$$

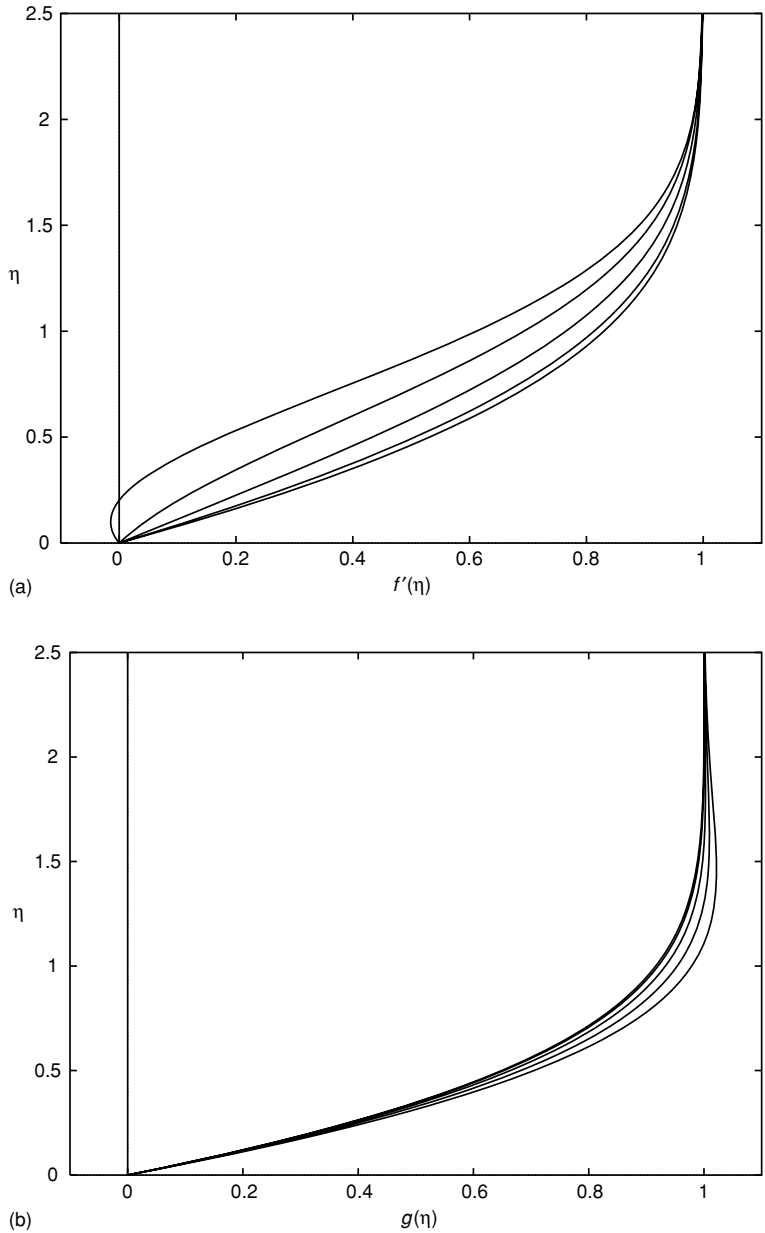

Figure 3.6 (a) The radial velocity function $f'(\eta)$ at a rotational stagnation point. Successive profiles from the lowest, which corresponds to the classical Homann flow, have $\Omega/k = 0.0(0.5)2.0$. (b) The azimuthal velocity function $g(\eta)$ corresponding to (a).

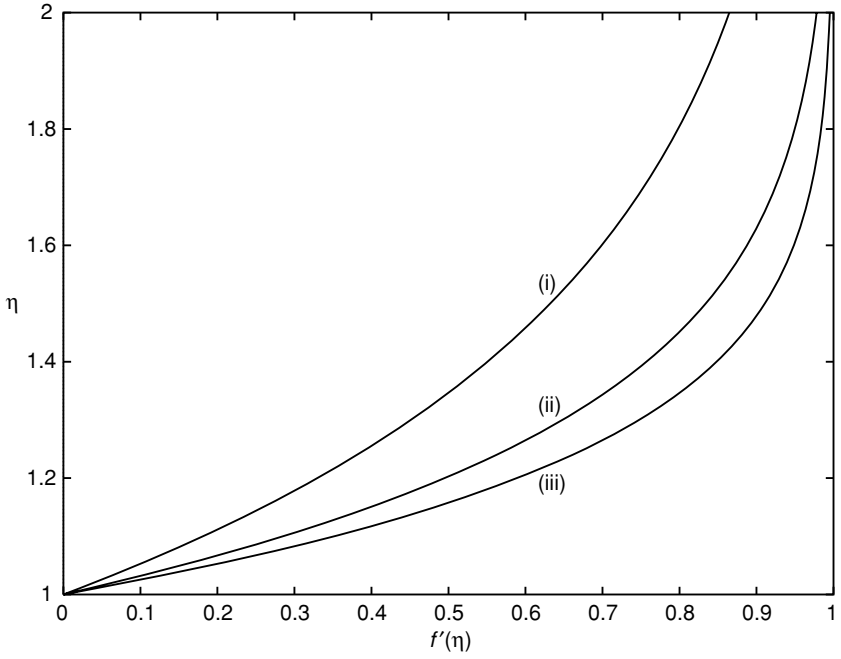

Figure 3.7 Profiles of the axial velocity function $f'(\eta)$ for stagnation flow on a circular cylinder. (i) $R = 2$, (ii) $R = 6$, (iii) $R = 10$.

For a viscous fluid we may write the Stokes stream function for this rotationally symmetric flow as

$$\psi = ka^2 z f(\eta) \quad \text{where} \quad \eta = (r/a)^2, \tag{3.26}$$

so that, from equation (1.24), we have the velocity components

$$v_r = -ka\eta^{-1/2} f(\eta) \quad \text{and} \quad v_z = 2kz f'(\eta). \tag{3.27}$$

Substituting into equations (1.19) and (1.20) gives, as the equation for f,

$$\eta f''' + f'' + R(ff'' - f'^2 + c) = 0, \tag{3.28}$$

where $R = ka^2/2\nu$ is a Reynolds number, and for the pressure

$$\frac{p - p_0}{\rho} = -\frac{1}{2}k^2 a^2 \eta^{-1} f^2(\eta) - 2\nu k f'(\eta) - 2k^2 z^2.$$

The boundary conditions for (3.28) require $f(1) = f'(1) = 0$, and for consistency with equation (3.25), $c = f'(\infty) = 1$. Equation (3.28) has been integrated numerically by Wang, and we present some such solutions in figure 3.7. We may note that as R increases a boundary-layer structure emerges. Indeed Wang

has shown that for $R \gg 1$ equation (3.28) may be transformed to the two-dimensional Hiemenz equation with relative error $O(R^{-1/2})$.

Burde (1994) has *inter alia*, also addressed this problem and finds an exact solution, for the case $R = 2$, as

$$f(\eta) = \tfrac{1}{2}\{2\eta + \mathrm{e}^{2(1-\eta)} - 3\},$$

which is included in figure 3.7.

Variations of this basic flow have been considered by several authors, Wang himself has considered the analogue of Crane's (1970) stretching plate problem. In that case the appropriate solution is still as in equations (3.26) and (3.27) with $f(\eta)$ satisfying (3.28), but now the boundary conditions are

$$f(1) = 0, \quad f'(1) = 1, \quad f'(\infty) = c = 0. \tag{3.29}$$

In obtaining numerical solutions, Wang draws attention to the difficulty in this case that solutions decay algebraically, rather than exponentially, as $\eta \to \infty$. Again Burde (1989) has found an exact solution in one particular case. In addition to the stretching cylinder, Burde introduces a uniform flow with speed U_∞ parallel to the generators of the cylinder. In that case equation (3.26) is replaced by

$$\psi = ka^2 z f(\eta) + U_\infty a^2 \int_0^\eta g(s)\,\mathrm{d}s.$$

The equation satisfied by $f(\eta)$ is again equation (3.28), with boundary conditions (3.29), whilst $g(\eta)$ satisfies

$$\eta g'' + g' + R(fg' - f'g) = 0, \tag{3.30}$$

with

$$g(1) = 0, \quad g(\infty) = \tfrac{1}{2}. \tag{3.31}$$

Burde notes that for the special case $R = 4/3$ there is an exact solution of each of equations (3.28) and (3.30), subject to (3.29) and (3.31) respectively, as

$$f(\eta) = 3\left(\frac{\eta - 1}{2\eta + 1}\right),$$

$$g(\eta) = \frac{4\eta^3 - 6\eta^2 - 4\eta + 1}{(2\eta + 1)^3} + \frac{3\ln\{(2\eta + 1)/3\} + 5/3}{(2\eta + 1)^2}.$$

Axial velocity profiles for this special case are shown in figure 3.8. Mention may also be made of the work of Gorla (1978) who, in the original problem of Wang (1974), allows the cylinder to slide parallel to its generators with uniform speed.

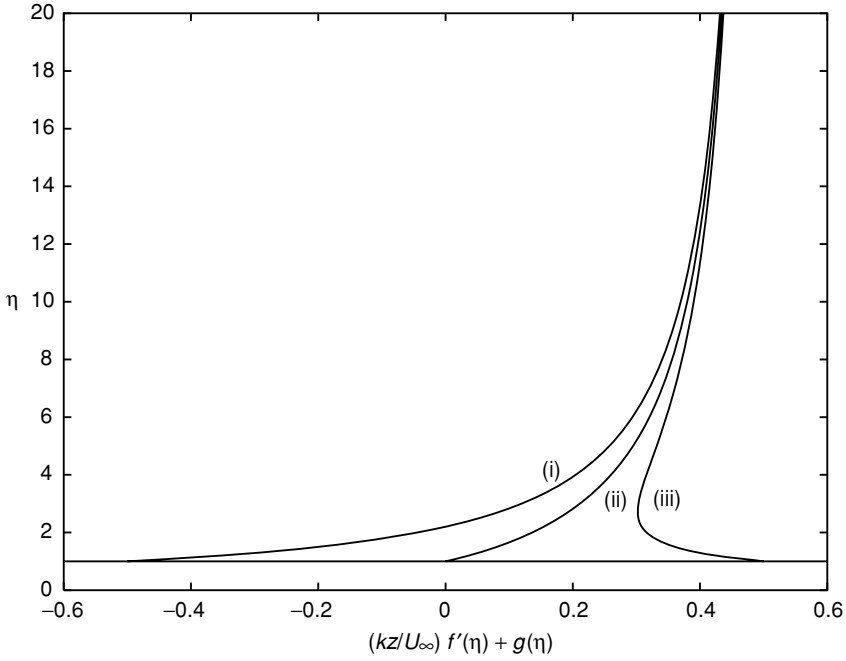

Figure 3.8 The axial velocity profile $v_z/2U_\infty = (kz/U_\infty)f'(\eta) + g(\eta)$ at a stretching cylinder in a uniform axial flow for $R = \frac{4}{3}$. (i) $kz/U_\infty = -\frac{1}{2}$, (ii) $kz/U_\infty = 0$, (iii) $kz/U_\infty = \frac{1}{2}$.

An analogue of the oblique stagnation-point flow considered in section 2.3.2 has been discussed by Weidman and Putkaradze (2003, 2005). In the far field the velocity components (3.25) are replaced by

$$v_r = -k\left(r - \frac{a^2}{r}\right), \quad v_z = 2kz + \gamma\left\{\left(\frac{r}{a}\right)^2 - 1\right\}.$$

The far-field vorticity is $-2\gamma r\hat{\boldsymbol{\theta}}$ and an additional term $4\gamma\nu z/a^2$ is required in the pressure field. Unlike the corresponding two-dimensional case, it should be noted that viscous effects are not negligible in the far field. Replacing (3.25) by

$$v_r = -ka\eta^{-1/2}f(\eta), \quad v_z = 2kzf'(\eta) + \gamma g(\eta),$$

and the corresponding pressure field by

$$\frac{p - p_0}{\rho} = -\frac{1}{2}k^2a^2\eta^{-1}f^2(\eta) - 2\nu kf'(\eta) - 2k^2z^2 + \frac{4\gamma\nu}{a^2}z,$$

where again $\eta = (r/a)^2$, then the equation for $f(\eta)$ is unchanged whilst, from (1.11), $g(\eta)$ satisfies

$$\eta g'' + g' + R(fg' - f'g) = 1, \quad \text{with} \quad g(0) = 0, \quad g'(\infty) = 1.$$

Solutions have been obtained by Weidman and Putkaradze (2005) for a range of values of R.

In a further development Cunning, Davis and Weidman (1998) elaborate upon the solution of Wang (1974) by both introducing uniform transpiration V_0 at the cylinder surface, and allowing it to rotate with constant angular velocity Ω. The solution is of the form (3.26) where $f(\eta)$ satisfies (3.28), supplemented by the azimuthal velocity

$$v_\theta = \Omega a \eta^{-1/2} h(\eta)$$

where $h(\eta)$ satisfies, from equation (1.20),

$$\eta h'' + Rfh' = 0, \tag{3.32}$$

and the pressure is now given by

$$\frac{p - p_0}{\rho} = -\frac{k^2 a^2 f(\eta)}{2\eta} - 2\nu k f'(\eta) - 2k^2 z^2 + \frac{\Omega^2 a^2}{2} \int_1^\eta \frac{g^2(s)}{s^2} \mathrm{d}s.$$

The boundary conditions for equations (3.28) and (3.32) now require

$$f(1) = -S, \quad f'(1) = 0, \quad f'(\infty) = 1, \quad h(1) = 1, \quad h(\infty) = 0, \tag{3.33}$$

where the transpiration parameter $S = V_0/ka$. For the case in which there is no rotation, $\Omega \equiv 0$, Burde (1994) has again presented exact solutions of equation (3.28) for $R = 2/(1 + S)$ as

$$f(\eta) = \eta - \tfrac{3}{2}(1 + S) + \tfrac{1}{2}(1 + S)\, \mathrm{e}^{2(1-\eta)/(1+S)}.$$

Although this solution encompasses a wide range of values of R and S, the two parameters cannot be prescribed independently. Cunning *et al.* (1998) have solved equation (3.28) numerically and, simultaneously, equation (3.32), subject to the conditions (3.33) for a wide range of values of the parameters R and S. Of particular interest are the solutions for strong blowing, $S \gg 1$ with R fixed. The flow structure that develops is one in which the axial profile $f'(\eta)$ thickens without change of character. However, the swirling velocity component, within the surface of zero radial velocity which itself increases in radius linearly with S, exhibits the character of a potential vortex. At the surface of zero radial velocity this is destroyed and the swirl decays rapidly to zero across a viscous layer of thickness $O\{(RS)^{-1/2}\}$.

3.4.3 Flow inside a porous or stretching tube

For the case of a porous, or stretching, tube it is not unnatural to consider the flow induced within it, that is, the analogue of the flow between plates across which there is suction or injection, or which stretch as considered in section 2.4.1. In the planar case the Hiemenz transformation was seen to be appropriate for fully developed flow and it is Wang's transformation, as in equation (3.26), that is the starting point for our discussion of flow within the tube.

Consider first the case of a porous tube across whose boundary fluid is either sucked or injected. The ordinary differential equation for the fully developed flow was initially addressed numerically by Berman (1958b) and White (1962). The solutions indicated that for wall suction solutions were not always possible, suggesting that in those cases fully developed flow is not possible, and that where solutions were obtained a dual was always available. However, the most comprehensive and penetrating account which reveals the rich and complex structure of the flow has been given by Terrill and Thomas (1969). Following Terrill and Thomas we write the analogue of equations (2.52) and (2.53) for this axisymmetric flow as

$$\psi = a^2(U_0/2 - V\bar{z})f(\eta), \quad \eta = (r/a)^2, \tag{3.34}$$

where $\bar{z} = z/a$, V is the velocity of suction at the tube wall $r = a$ and U_0 is an arbitrary constant velocity at $\bar{z} = 0$, though it may be remarked that Terrill and Thomas also explore the possibility of a non-uniform axial velocity at $\bar{z} = 0$. With $\mu V/a$ as a scale for the pressure we have as the analogue of equation (2.53)

$$\bar{p} = \frac{p}{\rho V^2 R^{-1}} = 2f' - \frac{1}{2}R\eta^{-1}f^2 - 4\lambda\bar{z}^2 + 4\lambda U_0 V^{-1}\bar{z},$$

where $R = Va/\nu$ is the Reynolds number, positive when fluid is sucked from the tube, negative when fluid is injected into it, and λ is not determined *a priori*. The equation satisfied by $f(\eta)$ is, analogous to (2.54),

$$\eta f''' + f'' + \tfrac{1}{2}R(f'^2 - ff'') - \lambda = 0, \tag{3.35}$$

with boundary conditions

$$f(0) = 0, \quad \lim_{\eta\to 0}\eta^{1/2}f''(\eta) = 0, \quad f(1) = 1, \quad f'(1) = 0. \tag{3.36}$$

As in the case of plane boundaries four boundary conditions are required, since λ also has to be determined. The principal results of Terrill and Thomas are that for $2.3 < R < 9.1$ there cannot be a fully developed flow in the tube, as in equation (3.34), that for $R < 2.3$ and for $9.1 < R < 20.6$ there are two

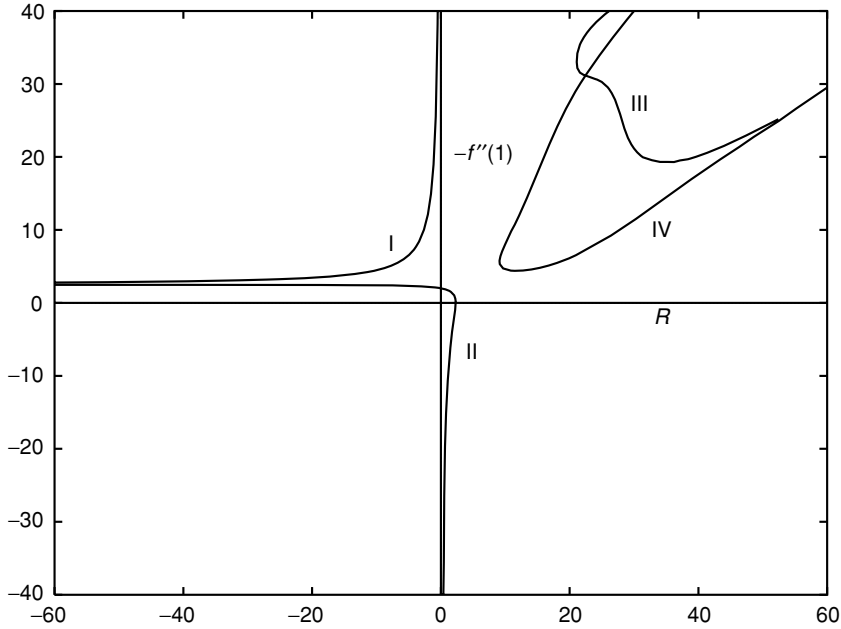

Figure 3.9 A map of the available solutions for flow within a porous tube in the $[-f''(1), R]$-plane. The solution groups I, II, III and IV are described in the text and illustrated below.

solutions. Skalak and Wang (1977) have extended the results of Terrill and Thomas and shown that for $R > 20.6$ there are four solutions. These results are shown in figure 3.9, where the variation of $-f''(1)$ is shown with Reynolds number R.

There are, essentially, four groups of solution corresponding to the four solution branches, and we consider each in turn with designations that differ from those of Terrill and Thomas. The solutions in Group I cover the whole range of injection Reynolds numbers. These solutions are characterised by a region of reversed flow in the central part of the tube. For large injection, the velocity profiles are unexceptional, but as $R \to 0-$ both the centre-line velocity $f'(0)$ and the wall shear stress $f''(1)$ tend to minus infinity. Examples of these Group I solutions are shown in figure 3.10.

On the lower branch of injection solutions in figure 3.9, designated Group II, $f'(\eta) > 0$ for all η with little variation in the profiles and with $f''(1)$ increasing. The further development on that solution branch shows R at first increasing into the suction regime, with a region of reversed flow developing in the wall region, and then decreasing. As $R \to 0+$ both the centre-line velocity and wall

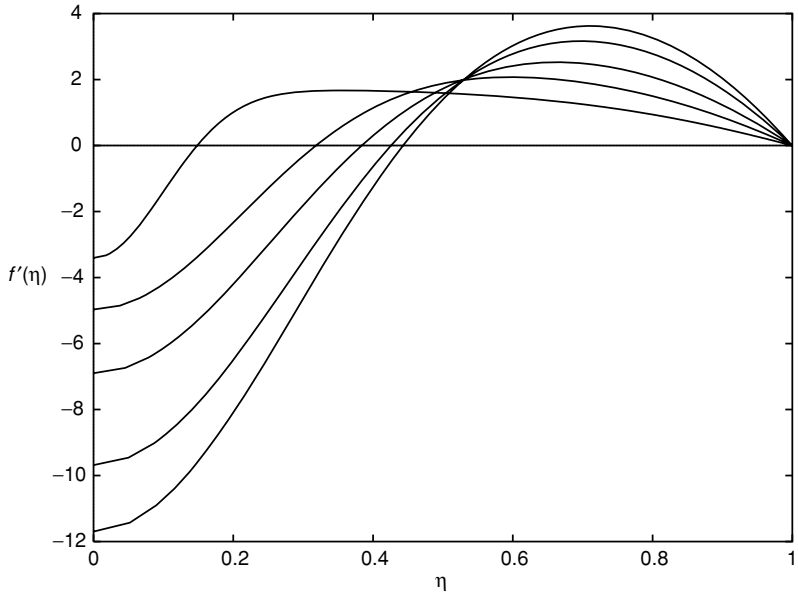

Figure 3.10 Velocity profiles $f'(\eta)$ corresponding to Group I in figure 3.9 with, from the lowest at $\eta = 0$: $R = -2.01, -2.61, -4.44, -8.83, -57.83$.

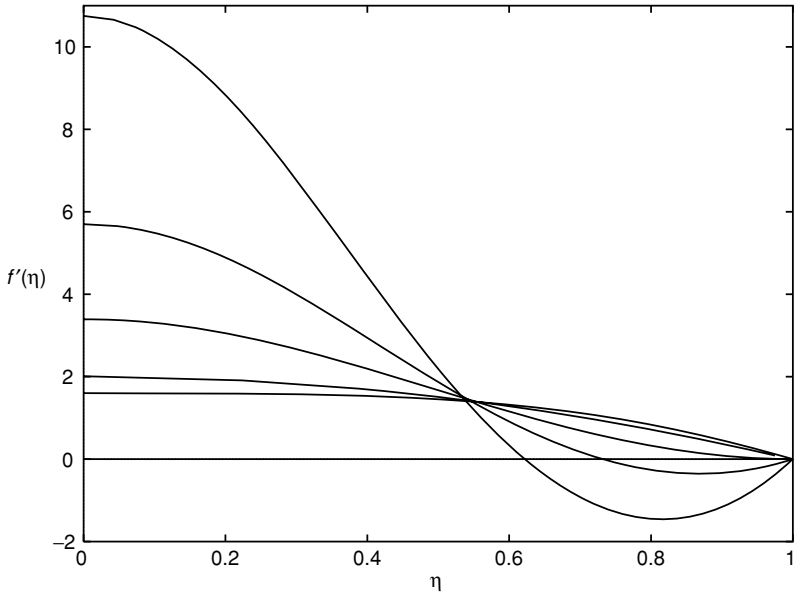

Figure 3.11 Velocity profiles $f'(\eta)$ corresponding to Group II in figure 3.9 with, from the lowest at $\eta = 0$: $R = -52.2, -0.04, 2.30, 1.93, 1.27$.

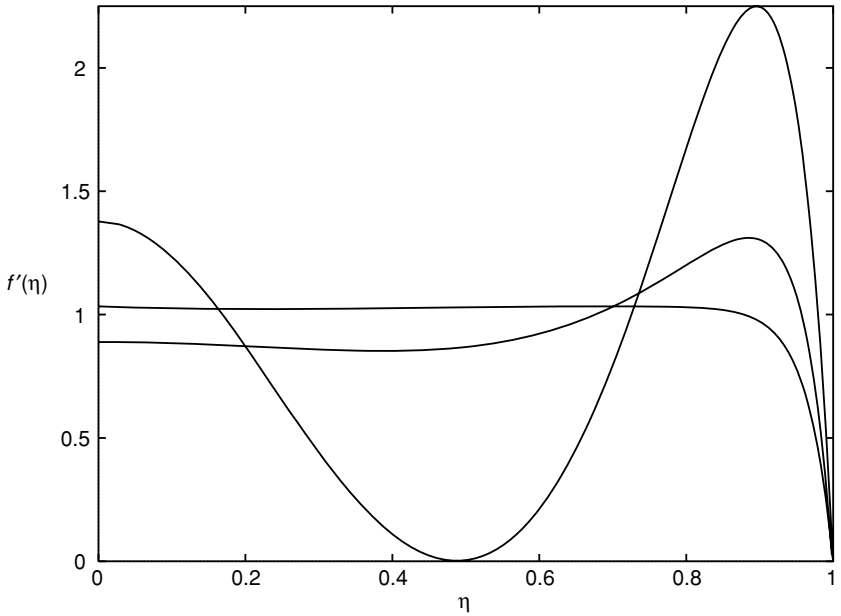

Figure 3.12 Velocity profiles $f'(\eta)$ corresponding to Group III in figure 3.9 with, from the lowest at $\eta = 0$: $R = 30.61, 60.0, 23.75$.

shear stress tend to infinity; typical profiles are shown in figure 3.11. Terrill and Thomas show that the suction and injection profiles of Group II and Group I, as $R \to 0\pm$ respectively, are the images of one another, reflected in the η-axis.

As already noted there is then a range of suction Reynolds numbers for which no solutions of equation (3.35) exist. Consider next the upper branch of solutions for $R > 0$, Group III. For $R \gg 1$ there is a core of uniform flow, with $f'(\eta) \approx 1$, flanked by a boundary layer of thickness $O(R^{-1})$. As R decreases the profile develops two points of inflection with local maxima close to the boundary and at the centre-line, with $f'(\eta) \lessgtr 1$ respectively, and a minimum between them; further decrease in R shows $f'(0)$ increasing to values greater than unity with the maximum close to $\eta = 1$ increasing and the minimum between them dipping below zero. Examples are shown in figure 3.12.

Finally there are Group IV solutions corresponding to the lower branch of suction solutions in figure 3.9. For $R \gg 1$ these are virtually indistinguishable from those of Group III. As R decreases the centre-line velocity at first increases and then decreases until for $R \approx 10$ there is reversed flow on the centre-line. Meanwhile close to the boundary the velocity increases. This development continues beyond the minimum value $R = 9.1$ and as R again increases on the

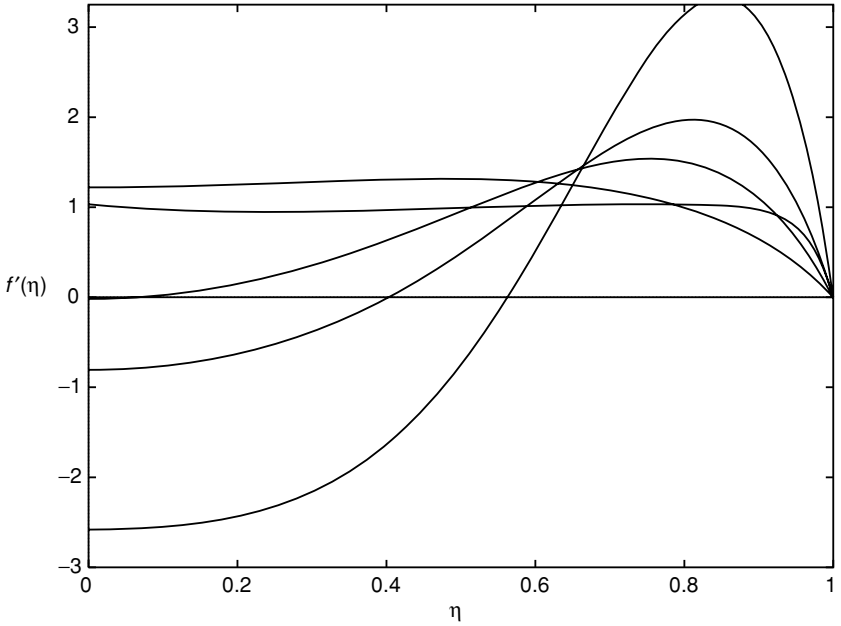

Figure 3.13 Velocity profiles $f'(\eta)$ corresponding to Group IV in figure 3.9 with, from the lowest at $\eta = 0$: $R = 21.6, 13.06, 10.04, 60.0, 13.83$.

upper part of this solution branch, until as $R \to 21.2$ the solution develops a positive maximum close to the centre-line. At $R = 21.2$ the solution is almost identical with that of Group III. A closer examination reveals, however, that as $R \to 21.2+$, $f''(0) \to \infty$ whilst as $R \to 21.1-$, $f''(0)$ remains finite. Velocity profiles for Group IV solutions are shown in figure 3.13.

As has been remarked the suction solutions of Groups III and IV are virtually indistinguishable for $R \gg 1$. Terrill and Thomas indicate that the two solutions differ by exponentially small terms. This difference is examined in more detail in a subsequent paper by Terrill (1973), who has also considered flow through a porous annulus (Terrill (1966)), extending the work of Berman (1958a). This annular flow problem has been extended by Marques, Sanchez and Weidman (1998) to include rotation, translation, stretching and twisting of the cylinders.

The absence of any solutions of equation (3.35), representing fully developed flow, in the range of Reynolds numbers $2.3 < R < 9.1$ has not been explained. Prager (1964) introduced a swirling component of velocity into the tube such that

$$v_\theta = (U_0 - 2V\bar{z})\eta^{-1/2} g(\eta),$$

with v_r, v_z again determined from the stream function (3.34). The equation satisfied by g is

$$\eta g'' + \tfrac{1}{2}R(f'g - fg') = 0$$

with $g(0) = 0$, $g(1) = 1$. This equation and that governing the axial flow, which now includes centrifugal effects, have been solved numerically by Terrill and Thomas (1973). Again there is a rich solution structure upon which we comment as follows. For injection, $R < 0$, there are two solutions, both with $f''(1) > 0$ and for both of which $f''(1) \to 0$ as $R \to 0$. For $R \lesssim -6$ these proved extremely difficult to determine and were not pursued. For suction, $R > 0$, there are dual solutions, with $f''(1) < 0$, in the range $0 < R \leq 9.7$ with only one solution for $R > 9.7$ which, as $R \to \infty$, becomes essentially identical with those of Groups III and IV in the absence of swirl. The differences are again attributed to exponentially small terms. The point of interest is, then, that the introduction of swirl into the tube leads to solutions of the fully developed flow equations for all values of $R > 0$. Though this sheds no light on why there should be a range of values of R in which no solutions are available in the absence of swirl.

As in the two-dimensional case of flow between porous or stretching plates there are some similarities between the flow driven by injection, discussed above, and the stretching tube flow considered by Brady and Acrivos (1981). With $\psi = U_0 a^2 \bar{z} f(\eta)$, and $\mu U_0/a$ again as a scale for the pressure, so that

$$\bar{p} = 4\lambda \bar{z}^2 - \left(2f' + \tfrac{1}{2}R\eta^{-1}f^2\right),$$

where $R = U_0 a/\nu$ and λ is undetermined, we now have as the equation for f,

$$\eta f''' + f'' + \tfrac{1}{2}R(ff'' - f'^2) - \lambda = 0, \tag{3.37}$$

together with

$$f(0) = 0, \quad \lim_{\eta \to 0} \eta^{1/2} f''(\eta) = 0, \quad f(1) = 0, \quad f'(1) = 1. \tag{3.38}$$

It is found numerically that equation (3.37), subject to (3.38), has no solutions in the range $10.25 < R < 147$. For $R < 10.25$ there are dual solutions. On one branch, as R increases from zero, $f'(0) < 0$ and decreases with $f'(\eta)$ increasing monotonically to $f'(1) = 1$ up to $R = 10.25$. As R decreases on the other branch from 10.25, $f'(0)$ decreases dramatically and is $O(R^{-1})$ as $R \to 0$. Simultaneously $f'(\eta)$ develops a maximum, close to the moving boundary, which itself increases dramatically as required by continuity.

These solutions for $R < 10.25$ are designated Group I. For $R > 147$ multiple solutions appear. Group II solutions are characterised for $R \gg 1$ by a boundary layer, thickness $O(R^{-1/2})$, at the moving boundary surrounding an inviscid core of uniform flow with $0 > f'(\eta) = O(R^{-1/2})$. As R decreases $f'(0)$ decreases until $R \approx 147$ whereupon R again increases, as does $f'(0)$, until $R = 186$ when $f'(0) = 0$. The Group III solutions are a continuation, with $f'(0)$ increasing with R, on this solution branch. On another solution branch there are again dual solutions designated Group IV. On one part of this branch when $R \gg 1$ the flow again consists of an inviscid core of zero vorticity surrounded by a conventional boundary layer. As R decreases on this solution branch the profile develops in a surprising manner such that for $R < 900$ there is a region of flow midway between the axis and the wall in which $f'(\eta) > 0$ flanked by regions with $f'(\eta) < 0$. This part of the solution branch ends at $R \approx 770$, and as R again increases on the other part the development described above continues with three different regions of flow in the core, in each of which the velocity increases with R, flanked by a boundary layer at the moving wall. In all cases, for $R > 147$, the values of $f''(1)$ are virtually indistinguishable.

Following Terrill and Thomas (1973), Brady and Acrivos introduce swirl into the tube and demonstrate the existence of dual solutions for all $R > 0$. However, as with the porous tube, this sheds no further light on the 'gap' range of Reynolds numbers when swirl is absent.

The flow outside a stretching tube has been considered by Wang (1988).

3.5 Rotating-disk flows

When a finite disk rotates in its own plane about an axis through its centre, in a fluid otherwise at rest, fluid is centrifuged radially and thrown off the perimeter in a jet-like manner, a phenomenon that is easily realised experimentally. As a model for this an infinite rotating disk was first studied by von Kármán (1921), and by Cochran (1934). Subsequently, extensions of this basic flow were proposed by Hannah (1947) who considered forced flow against the rotating plane, Batchelor (1951) who allowed solid-body rotation of the fluid in the main body of fluid beyond the plane and Stuart (1954) who considered the effect of uniform suction at it, when assumed porous. In a related situation a stationary plane is placed in a fluid otherwise in solid-body rotation; this was first discussed by Bödewadt (1940); whilst Batchelor (1951) studied the flow bounded by two disks, both of which were allowed to rotate. It is convenient to consider the one- and two-disk situations separately.

3.5.1 The one-disk problem

We concentrate on the axisymmetric flow first proposed by von Kármán, but we also consider a non-axisymmetric flow discovered by Hewitt, Duck and Foster (1999).

As with the stagnation-point flows considered in section 3.4 there is no natural length scale in this problem and a self-similar solution is available. Again utilising cylindrical polar co-ordinates with the rotating plane, angular velocity Ω, coinciding with $z = 0$, and the axis of rotation taken as $r = 0$, the velocity components may be written as

$$v_r = r\Omega f'(\eta), \quad v_\theta = r\Omega g(\eta), \quad v_z = -2(\nu\Omega)^{1/2} f(\eta), \quad \eta = \left(\frac{\Omega}{\nu}\right)^{1/2} z, \tag{3.39}$$

and the pressure as

$$\frac{p - p_0}{\rho} = \frac{1}{2} r^2 \Omega^2 \lambda - 2\nu\Omega(f^2 + f'). \tag{3.40}$$

Equations (1.19), (1.20) then yield, as equations for f and g,

$$f''' + 2ff'' - f'^2 + g^2 = \lambda, \tag{3.41}$$

$$g'' + 2(fg' - f'g) = 0, \tag{3.42}$$

with boundary conditions

$$f(0) = \lambda_1, \quad f'(0) = 0, \quad g(0) = 1, \quad f'(\infty) = \lambda_2, \quad g(\infty) = \lambda_3. \tag{3.43}$$

In these equations we recover the classical von Kármán flow by setting $\lambda = \lambda_i = 0$ $(i = 1, 2, 3)$. Von Kármán himself derived an approximate method of solution, whilst the first adequate numerical solution was presented by Cochran using appropriate series expansions for large and small values of η. This classical solution is shown in figure 3.14; it clearly reveals the radial flow associated with centrifugal effects.

Stuart (1954) extended Cochran's numerical work to include the effect of suction at a porous disk with $\lambda_1 = 1$; this solution is also shown in figure 3.14 where we see the fluid is literally 'sucked' towards the disk when compared with the classical case. Stuart also presented a series solution in descending powers of λ_1.

With $\lambda = -(k/\Omega)^2$, $\lambda_2 = k/\Omega$, $\lambda_1 = \lambda_3 = 0$, the problem is formulated as by Hannah for the case of flow towards the rotating disk such that at large distances from it $v_r = kr$, $v_\theta = 0$, $v_z = -2kz$, as in the classical stagnation-point flow. Hannah calculated a few solutions for this case, whilst Tifford and Chu (1952) extended the range. One such solution is included in figure 3.15, showing a 'squeezing' of the flow towards the rotating plane. An extension of this to a case in which the onset flow is of saddle-point type, rather than

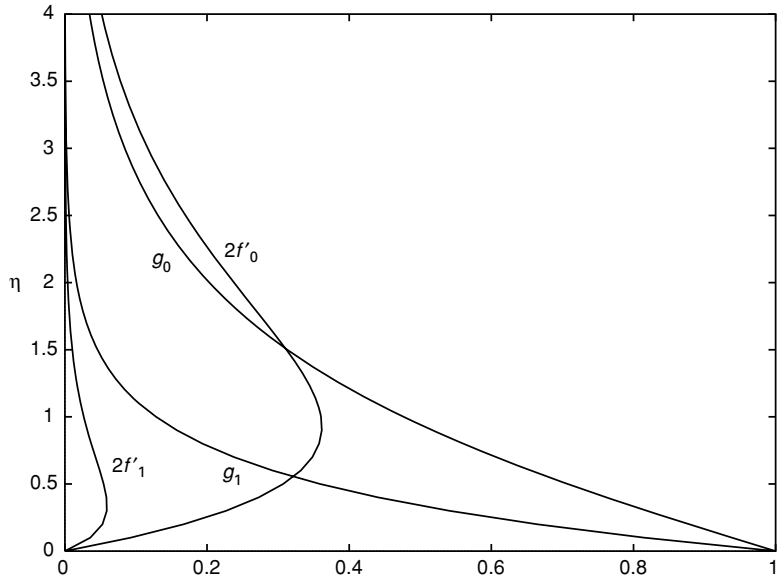

Figure 3.14 Rotating-disk flows. The radial and azimuthal velocity profiles $f_i'(\eta)$, $g_i(\eta)$ are shown for the classical von Kármán flow, $i = 0$, and for a case of suction at the boundary, $i = 1$, as considered by Stuart for $\lambda_1 = 1$.

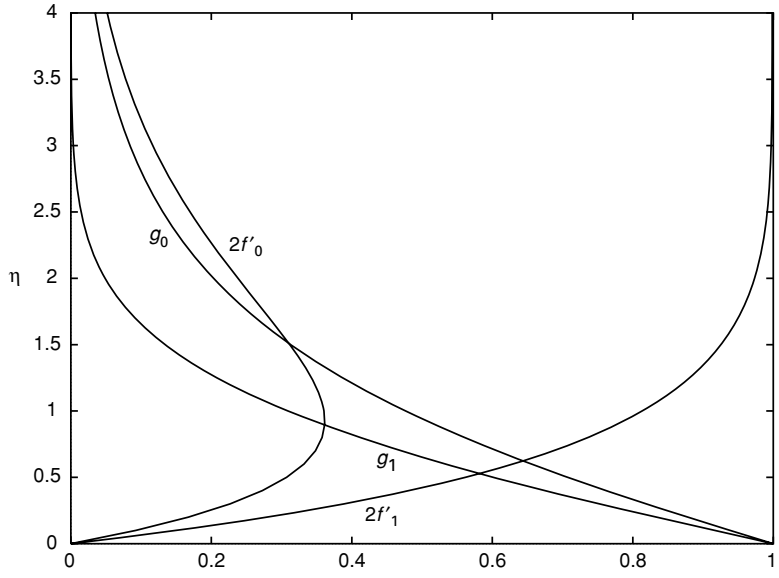

Figure 3.15 As for figure 3.14 except that now the case $i = 1$ corresponds to the case of flow towards the rotating disk, with $\lambda_2 = \frac{1}{2}$, as considered by Hannah.

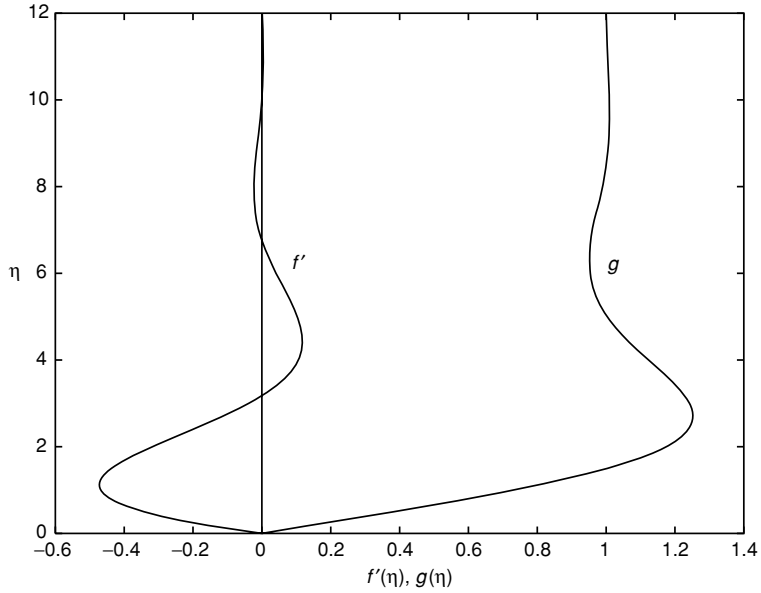

Figure 3.16 The case of solid-body rotation over a disk that is at rest; $f'(\eta)$, $g(\eta)$ are profiles of the radial and azimuthal velocity functions respectively.

axisymmetric stagnation flow, has been considered by Hall, Balakumar and Papageorgiu (1992).

Solutions with $\lambda_2 = 0,\ \lambda = s^2,\ \lambda_1 \neq 0,\ \lambda_3 = s$, have been extensively studied. Before considering these we note that the problem has attracted several rigorous approaches, and the work of McLeod (1971) deserves especial mention as the first to guarantee the existence of a solution for $s \geq 0$ and arbitrary values of λ_1, so including the classical von Kármán flow. For $s < 0$, McLeod has shown that no solution exists for $s = -1$ with $\lambda_1 = 0$ whilst Watson (1966) has established existence for $s = -1$ and λ_1 sufficiently large.

The first systematic study of equations (3.41) to (3.43) with $s \neq 0$ was carried out by Rogers and Lance (1960). With $\lambda_1 = 0$ they showed that as s increases from the classical solution with $s = 0$ the flow approaches the solid-body rotation at infinity in an oscillatory manner, with the exception $s = 1$ of course, when the whole flow is a solid-body rotation. As $s \to \infty$ the problem, suitably scaled, approaches that considered by Bödewadt where the disk is at rest in a fluid that rotates with uniform angular velocity at large distances from it. More directly, in terms of the formulation above, Bödewadt's problem is posed in equations (3.41) to (3.43) with $\lambda_1 = \lambda_2 = 0,\ \lambda = \lambda_3 = 1$ and the condition on g at $\eta = 0$ replaced by $g(0) = 0$. The solution for this case is shown in figure 3.16.

For $s < 0$ the situation proved to be more complex. The results obtained by Rogers and Lance suggested that in the absence of suction no solutions exist for $s \leq -0.2$. A subsequent investigation was carried out by Evans (1969) for $s < 0$. He was unable to obtain solutions in the range $-1.35 < s < -0.161$ in the absence of suction, but the introduction of sufficient suction did enable solutions to be calculated. A more detailed analysis has been carried out by Zandbergen and Dijkstra (1977) for $\lambda_1 = 0$ as $s \to -0.16+$. They found that the critical value of s at which the solution breaks down is $s_{cr} = -0.16053876$, where the solution $f(\eta; s)$ exhibits square-root singular behaviour such that $\partial f/\partial s \to \infty$ as $s \to s_{cr}$. They further unveiled a second solution branch which merges with the first at $s = s_{cr}$. This second branch was continued up to $s = 0.07452563$ where a third branch appeared. Subsequently Dijkstra and Zandbergen (1978) discovered an infinity of solution branches oscillating about $s = 0$. A representation of these may be found in Zandbergen (1980), or the comprehensive review article by Zandbergen and Dijkstra (1987). At $s = 0$, say, a characteristic feature of these solutions is associated with the following:

$$f(\eta) = -\alpha \sin^2\{\beta(\eta - \eta_0)\} - s/4\alpha\beta^2, \quad g = \pm 2\beta f. \tag{3.44}$$

It may be verified that for $\alpha \gg \beta$, $\alpha\beta \gg 1$, (3.44) represents a leading-order inviscid solution of equations (3.41) and (3.42), in the nature of a 'hump'. For each new solution branch Dijkstra and Zandbergen (1978) show that a new hump is added to the solution, four times larger than the last one on the preceding branch. Dijkstra (1980) analyses the viscous layers between successive humps.

This multiplicity of solutions in the neighbourhood of $s = 0$ does not exhaust the possibilities. Bodonyi (1975) calculated solutions for large negative s, and with increasing s showed that a breakdown of the solution occurs as $s \to -1.436$. Prior to that Ockendon (1972), allowing small values of suction ($\lambda_1 \ll 1$), constructed solutions in the range $|s| < 1.436$. Her results, which included multiple solutions again characterised by thick inviscid layers separated by thin viscous layers, suggested that as $\lambda_1 \to 0$ both of the values $s = \pm 1.436$ are rather special. Indeed whole families of solutions in the neighbourhood of $s = \pm 1.436$ have been constructed by Zandbergen (1980) for $\lambda_1 = 0$, and a summary representation is presented both there and by Zandbergen and Dijkstra (1987).

The above discussion has centred solely on axisymmetric flows. However, Hewitt, Duck and Foster (1999) have discovered that a non-axisymmetric

solution is available, associated with the still axisymmetric boundary conditions. With

$$v_r = r\Omega\{f'(\eta) + \phi(\eta)\cos 2\theta\}, \quad v_\theta = r\Omega\{g(\eta) - \phi(\eta)\sin 2\theta\},$$
$$v_z = -2(\nu\Omega)^{1/2} f(\eta),$$

where η is as before, and the pressure is given by equation (3.40) with $\lambda = s^2$, we have from equations (1.19) and (1.20),

$$f''' + 2ff'' - f'^2 - \phi^2 + g^2 = s^2,$$

$$g'' + 2(fg' - f'g) = 0, \quad \phi'' + 2(f\phi' - f'\phi) = 0,$$

together with boundary conditions

$$f(0) = f'(0) = \phi(0) = 0, \quad g(0) = 1, \quad f'(\infty) = \phi(\infty) = 0, \quad g(\infty) = s.$$

A numerical investigation has yielded non-axisymmetric solutions for values of s on the interval $-0.14485 \leq s \leq 0$. Hall, Balakumar and Papageorgiu (1992) have also investigated non-axisymmetry of the above type. For the most part they are concerned with unsteady flow, as discussed in chapter 5.

Axial symmetry of the flow is also compromised if there is a non-axisymmetric flow over the disk. Rott and Lewellen (1967) have considered, in particular, cases in which there is a uniform stream over the rotating plane, or the plane is in pure translation adjacent to a rotating fluid; Wang (1989b) considers the case of a shear flow over a rotating plane.

Whilst the exact solutions described above relate to the rotation of an infinite disk they do find application to a finite disk of radius a, say, as long as radial outflow is maintained. In that case, if $R_a = \Omega a^2/\nu \gg 1$, the effect of the edge is localised to its neighbourhood and the flow otherwise is as described by the above exact solutions. Advantage has been taken of this by, for example, Langlois (1985) and Riley (1987) in their models of the crystal/melt interface associated with the Czochralski crystal growth process.

3.5.2 The two-disk problem

For the problem of two disks, separated by a distance h, say, the representations (3.39) and (3.40) may still be used, but the boundary conditions are now applied at $\eta = (\Omega/\nu)^{1/2}h = R^{1/2}$ where $R = \Omega h^2/\nu$ is the Reynolds number. It proves convenient to write $\eta = R^{1/2}\zeta$, $f = R^{1/2}F$, $g = G$ so that equations

(3.41), (3.42) become, with a prime now denoting differentiation with respect to ζ,

$$R^{-1}F''' + 2FF'' - F'^2 + G^2 = \lambda, \tag{3.45}$$

$$R^{-1}G'' + 2(FG' - F'G) = 0, \tag{3.46}$$

together with, for impermeable disks,

$$F(0) = F'(0) = 0, \quad G(0) = 1, \quad F(1) = F'(1) = 0, \quad G(1) = s, \tag{3.47}$$

and the pressure is given by

$$\frac{p - p_0}{\rho} = \frac{1}{2}\lambda r^2\Omega^2 - 2\nu\Omega(RF^2 + F'). \tag{3.48}$$

There are six boundary conditions, (3.47), for the fifth-order system (3.45), (3.46), but as with other confined systems that have been encountered, the pressure is only determined to within the unknown constant λ which emerges from the solution procedure.

The first serious attempts to understand the flow were made by Batchelor (1951) and Stewartson (1953). For the case $s \geq 0$ Batchelor argued that for $R \gg 1$, the fluid in the core would rotate with constant angular velocity, with boundary layers at each disk. The latter would be as in the appropriate one-disk family of solutions. For counter-rotating disks with $s = -1$, Batchelor argued that in the core, when $R \gg 1$, there would be two regions of uniform, counter-rotating flow, separated by a shear layer at $\zeta = 1/2$, with boundary layers at each disk. However, Stewartson (1953) challenged these conjectures for $s = 0, -1$ and predicted that the fluid in the core would not rotate at all for large R, with boundary layers at each disk.

These matters remained unresolved until some light was shed on them by Lance and Rogers (1962). For $s = 0, 0.5$ numerical solutions of equations (3.45) to (3.47) were obtained up to $R = O(10^2)$. As R increases the flow development in each case is the same. Boundary layers develop on each disk with inflow on the slower, outflow on the faster, which flank a core flow of uniform angular velocity as predicted by Batchelor. The solutions obtained are consistent with single-disk solutions at each disk, with the same axial velocity at the edge of the boundary layer. For $s = -0.3$ the solutions obtained by Lance and Rogers again show an emerging core flow with uniform angular velocity, but now the emerging double boundary-layer structure on the faster rotating disk precludes the possibility of a construction from the single-disk solutions. In the case where the disks have equal and opposite angular velocities, $s = -1$, solutions were obtained up to $R = O(10^3)$. The flow which is emerging has the

main body of fluid at rest except for a slow, uniform inward drift to supply the slow axial motion from the plane of symmetry towards the disks, essentially as proposed by Stewartson. Subsequent rigorous analysis by McLeod and Parter (1974) established the existence of a Stewartson-type solution for $s = -1$, but throws no light on uniqueness or otherwise. Meanwhile Pearson (1965), by integrating their unsteady analogues, achieved steady-state solutions of equations (3.45) to (3.47) for $s = 0$ and $R = 1000$ confirming the existence of a Batchelor-type solution. But for the counter-rotating case $s = -1$ at $R = 1000$ a solution which is not antisymmetric about the centre-line $\zeta = 1/2$ emerges, and is therefore different from both the Batchelor–Stewartson proposals, and the calculated solutions of Lance and Rogers. The structure of the solution, which has been further investigated by Tam (1969), provides evidence for emerging inviscid structures of the type shown in equation (3.44). This evidence of non-uniqueness from the work of Pearson was followed by the landmark paper of Mellor, Chapple and Stokes (1968) for the case $s = 0$. For $R \gtrsim 200$ they not only found numerical solutions of both Batchelor and Stewartson type, but in addition solutions incorporating two or three cells of the form shown in equation (3.44). Some years later Kreiss and Parter (1983), by rigorous analytical means, established existence and non-uniqueness of solutions for all s when R is sufficiently large. Meanwhile several authors were extending the earlier solutions of Lance and Rogers to higher values of R. For example Pesch and Rentrop (1978) calculated the counter-rotating case $s = -1$ up to $R = 20000$ with the Stewartson solution clearly emerging. For $s = 0$, Wilson and Schryer (1978), with values of the Reynolds number up to $R = 10000$, show clearly a Batchelor-type solution with a now extensive region in the core where the angular velocity is uniform with value 0.3131Ω. Wilson and Schryer also allow suction at the rotating disk; the Batchelor-type solution persists with a uniform angular velocity in the core which increases with the suction rate. Keller and Szeto (1980) calculate the flow for $-1 < s < 1$ up to $R = 1000$. They conclude, in particular, that the solution is unique for $R \lesssim 55$.

The emergence of hump-like structures of the form (3.44) in the multiple solutions of Mellor *et al.* suggests, from experience with the single disk, that the complete solution space is very complex. This is highlighted by the work of Holodniok, Kubicek and Hlavacek (1981) who carried out calculations at $R = 625$ for $|s| \leq 1$. The relationship between the constant λ in equation (3.45) and s, also reproduced by Zandbergen and Dijkstra (1987), shows that no fewer than twenty solution branches have been identified.

In the above situations both disks rotate co-axially around the common axis $r = 0$, about which the flow has been assumed symmetrical. Unexpectedly, an exact solution of the Navier–Stokes equations is also available between infinite

parallel planes that each rotate with angular velocity Ω about different axes. This was identified by Berker (1963), rediscovered by Abbot and Walters (1970), and further discussed by Berker (1982).

With the disk at $z = 0$ rotating about $x = 0$, $y = -l$, and that at $z = h$ about $x = 0$, $y = l$ the boundary conditions require, at $z = 0$,

$$v_r = -\Omega l \cos\theta, \quad v_\theta = \Omega(r + l\sin\theta), \quad v_z = 0, \tag{3.49}$$

and at $z = h$,

$$v_r = \Omega l \cos\theta, \quad v_\theta = \Omega(r - l\sin\theta), \quad v_z = 0. \tag{3.50}$$

The nature of the boundary conditions suggests a solution of the form

$$\begin{aligned} v_r &= \Omega l\{f(\eta)\cos\theta + g(\eta)\sin\theta\}, \\ v_\theta &= \Omega r + \Omega l\{g(\eta)\cos\theta - f(\eta)\sin\theta\}, \quad v_z = 0, \end{aligned} \tag{3.51}$$

where $\eta = z/h$, which satisfies the continuity equation identically. With the pressure given by $p - p_0 = \rho\Omega^2 r^2/2$, equations (1.19), (1.20) yield the following, linear, equations for f and g,

$$f'' + Rg = 0, \quad g'' - Rf = 0, \quad \text{where again} \quad R = \Omega h^2/\nu, \tag{3.52}$$

together with, from (3.49) and (3.50), the boundary conditions

$$f(0) = -1, \quad g(0) = 0, \quad f(1) = 1, \quad g(1) = 0. \tag{3.53}$$

The solutions of equations (3.52), subject to (3.53), with $\alpha = (R/2)^{1/2}$, are

$$\begin{aligned} f = {} & [\{\sinh\alpha\eta\cos\alpha\eta + \sinh\alpha(\eta-1)\cos\alpha(\eta-1)\}\sinh\alpha\cos\alpha \\ & + \{\cosh\alpha\eta\sin\alpha\eta + \cosh\alpha(\eta-1)\sin\alpha(\eta-1)\}\cosh\alpha\sin\alpha]/ \\ & (\sinh^2\alpha\cos^2\alpha + \cosh^2\alpha\sin^2\alpha), \end{aligned}$$

$$\begin{aligned} g = {} & [\{\cosh\alpha\eta\sin\alpha\eta + \cosh\alpha(\eta-1)\sin\alpha(\eta-1)\}\sinh\alpha\cos\alpha \\ & - \{\sinh\alpha\eta\cos\alpha\eta + \sinh\alpha(\eta-1)\cos\alpha(\eta-1)\}\cosh\alpha\sin\alpha]/ \\ & (\sinh^2\alpha\cos^2\alpha + \cosh^2\alpha\sin^2\alpha). \end{aligned}$$

The solution implies that each plane $\eta = \eta_0$, $0 < \eta_0 < 1$ rotates as if rigid, with angular velocity Ω, about an axis $x_0 = -lg(\eta_0)$, $y_0 = lf(\eta_0)$. The locus of such points is a straight line only in the limit $R = 0$. In figure 3.17 we show the projection of this locus on the (x, y)-plane for various values of the Reynolds number.

Rotating-disk flows find application in viscometry. Abbot and Walters were concerned, in particular, with a theoretical understanding of the then recently

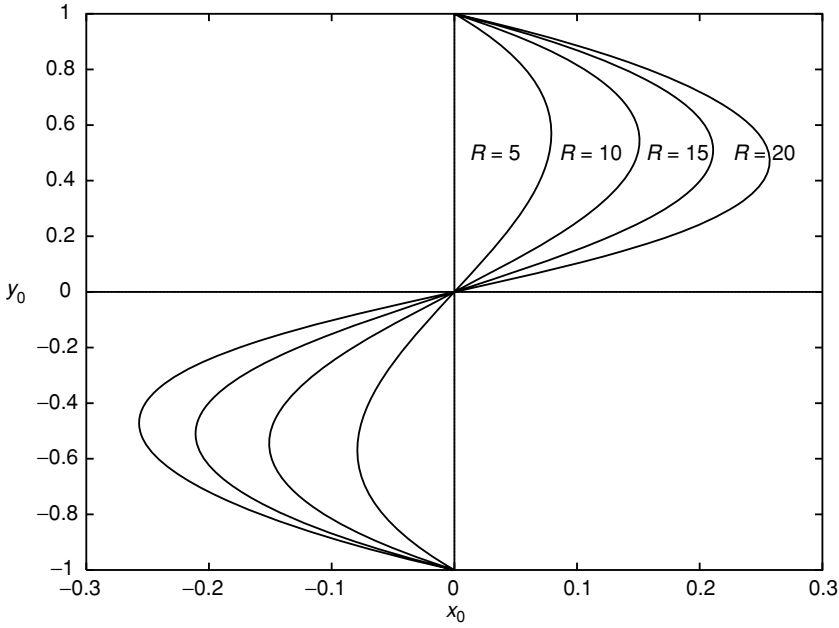

Figure 3.17 Projection onto the (x, y)-plane of the locus of points in $0 \leq z/h \leq 1$, for various values of R, about which rigid rotation takes place, between off-set rotating planes at $z/h = 0, 1$.

introduced orthogonal rheometer to determine the complex viscosity of an elastico-viscous liquid.

3.6 Ekman flow

A flow not unrelated to the above involves streaming across a single rotating plane in an otherwise unbounded fluid, which itself is in almost solid-body rotation with angular velocity $\boldsymbol{\Omega} = \Omega\mathbf{k}$. If the Navier–Stokes equations are written in a frame of reference that rotates with that same angular velocity then, if $\mathbf{v}^*$ now denotes fluid velocity relative to the rotating frame we have, for steady flow,

$$(\mathbf{v}^*.\nabla)\mathbf{v}^* + 2\boldsymbol{\Omega} \wedge \mathbf{v}^* = -\frac{1}{\rho}\nabla p^* + \nu\nabla^2\mathbf{v}^*, \quad \nabla.\mathbf{v}^* = 0, \tag{3.54}$$

where in (3.54) p^* now denotes the reduced pressure incorporating as it does the centrifugal term $\boldsymbol{\Omega} \wedge (\boldsymbol{\Omega} \wedge \mathbf{r})$. If in this rotating frame $\mathbf{v}^* = (u^*_\infty, v^*_\infty, 0)$ is constant at large distances from the plane boundary then the solution of

(3.54) will be of the form $\mathbf{v}^* = \{u^*(z), v^*(z), 0\}$ with $p^* = p^*(x, y)$ such that $\partial p^*/\partial x = 2\rho\Omega v^*_\infty$, $\partial p^*/\partial y = -2\rho\Omega u^*_\infty$ and u^*, v^* satisfying

$$\nu\frac{\partial^2 u^*}{\partial z^2} + 2\Omega(v^* - v^*_\infty) = 0, \quad \nu\frac{\partial^2 v^*}{\partial z^2} - 2\Omega(u^* - u^*_\infty) = 0. \tag{3.55}$$

In the rotating frame of reference $u^* = v^* = 0$ at $z = 0$ and the solution of (3.55) is, then,

$$u^* = u^*_\infty - \mathrm{e}^{-\eta}(u^*_\infty \cos\eta + v^*_\infty \sin\eta), \quad v^* = v^*_\infty - \mathrm{e}^{-\eta}(v^*_\infty \cos\eta - u^*_\infty \sin\eta),$$

where $\eta = (\Omega/\nu)^{1/2} z$. The velocity $\mathbf{v}^*$ so determined moves on a spiral as η increases known as the Ekman spiral following the pioneering work of Ekman (1905) in the field of rotating fluid flow dynamics.

3.7 Concentrated flows: jets and vortices

3.7.1 The round jet

Jets are characterised by the momentum flux within them stimulated, for example, by the application of a force at some given point. If M_c is a component of momentum flux across a sphere of radius r then M_c/ρ has dimensions L^4T^{-2}, the only other parameter involved, the kinematic viscosity ν, has dimensions L^2T^{-1} and so, since no natural length or time scales are involved, a solution of similarity form may be anticipated. This, rather than the more obvious flow in a cone, may be considered as the analogue of the Jeffery–Hamel flow discussed in chapter 2.

Using spherical polar co-ordinates, and assuming the flow is independent of ϕ, the stream function may be written as

$$\psi = \nu r f(\eta) \quad \text{where} \quad \eta = \cos\theta, \tag{3.56}$$

so that the velocity components are

$$v_r = \frac{\nu}{r} f'(\eta) \quad \text{and} \quad v_\theta = \frac{\nu}{r}\frac{f(\eta)}{(1-\eta^2)^{1/2}}. \tag{3.57}$$

If the pressure is written as

$$\frac{p - p_0}{\rho} = \frac{\nu^2}{r^2} P(\eta), \tag{3.58}$$

then introducing (3.57) and (3.58) into equation (1.26) yields for P, following integration,

$$P = -\frac{1}{2}\frac{f^2}{1-\eta^2} + f' + k_1, \tag{3.59}$$

where k_1 is a constant of integration. Substituting (3.57), (3.58) and (3.59) into equation (1.25) and integrating twice gives, as equation for f,

$$\tfrac{1}{2}(1-\eta^2)f' + \tfrac{1}{4}f^2 + \eta f + \tfrac{1}{2}k_1\eta^2 + k_2\eta + k_3 = 0, \tag{3.60}$$

where k_2, k_3 are arbitrary constants.

Yatseyev (1950) has obtained the general solution of equation (3.60), an equation first derived by Slezkin (1934). Application to the round jet was first discussed by Landau (1944), and subsequently in more detail by Squire (1951, 1952, 1955). The first point to note is that if $\eta = 1$, that is $\theta = 0$, is taken as the jet axis then $f(1) \equiv 0$ and so if $f'(1)$, and hence the radial velocity on the axis, are to be finite it is necessary to set $k_1 = -k_2 = 2k_3 = -2k$, say, so that the last three terms of (3.60) become $-k(1-\eta)^2$. Several special cases are worthy of attention.

(i) $k = 0$. In this case the solution is, with a an arbitrary constant,

$$f = -\frac{2(1-\eta^2)}{a+1-\eta}, \quad \text{so that} \quad f' = \frac{4a\eta - 2(\eta-1)^2}{(a+1-\eta)^2}, \tag{3.61}$$

from which we have $v_r|_{\theta=0} = 4\nu/ar$. The solution (3.61) is appropriate to a round jet in an unbounded fluid due to a point force, that is a source of momentum, at the origin. By considering the flux of x-momentum, M_x, across a sphere of radius r Squire (1951) has shown that $a = a(M_x)$ may be calculated from

$$\frac{M_x}{2\pi\rho\nu^2} = \frac{32(1+a)}{3a(2+a)} + 8(1+a) - 4(1+a)^2 \ln\left(\frac{2+a}{a}\right),$$

so that, in particular, as $a \to 0$,

$$\frac{M_x}{2\pi\rho\nu^2} \sim \frac{16}{3a} + 4\ln a.$$

Streamline patterns for this flow are shown in figure 3.18.

It is interesting to note that the theoretical results for the round laminar jet agree well with the experimental results for a turbulent jet, see Hinze and van der Hegge Zijnen (1949). For the turbulent jet ν must be taken as an eddy viscosity, and the good agreement suggests that for jet-like flows the assumption of a constant eddy viscosity is a good one.

(ii) $k = -(1+4b^2)/4$. For this second case, considered by Squire (1952), the boundary condition $f = 0$ is imposed at both $\eta = 1$ and $\eta = 0$ so that the plane $\theta = \pi/2$ may be considered as a solid boundary. The appropriate solution is

$$f = -\frac{(1+4b^2)(1-\eta)}{2b\cot\{b\ln(1+\eta)\} - 1},$$

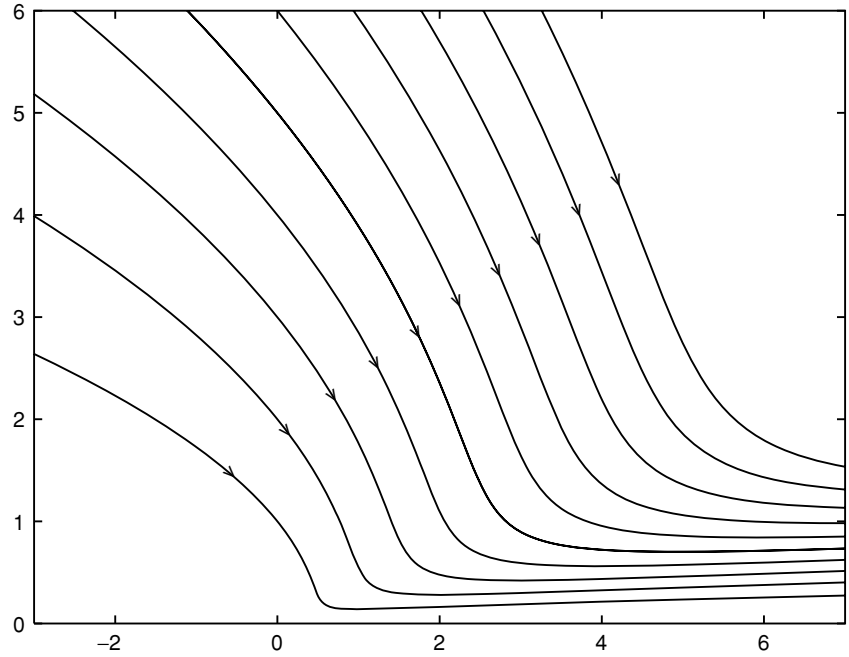

Figure 3.18 Streamlines for an unbounded round jet due to a point source of momentum, from equation (3.61) with $a = 0.01$.

so that

$$f' = \frac{1+4b^2}{2b\cot\{b\ln(1+\eta)\}-1}\left[1-2b^2\left(\frac{1-\eta}{1+\eta}\right)\frac{\operatorname{cosec}^2\{b\ln(1+\eta)\}}{2b\cot\{b\ln(1+\eta)\}-1}\right],$$

with

$$f'(1) = \frac{1+4b^2}{2b\cot(b\ln 2)-1}, \quad f'(0) = -\frac{1}{2}(1+4b^2).$$

Thus, although $v_\theta = 0$ on $\theta = \pi/2$, $v_r \neq 0$ and the solution suffers from the drawback that it does not satisfy the no-slip condition at the plane boundary from which the jet originates at $r = 0$. Narrow high-speed jets correspond to values of b for which $2b\cot(b\ln 2) \approx 1$; an example is shown in figure 3.19.

(iii) $k_1 = k_2 = 0, k_3 = 1 - b^2$. This case, unlike the two previous examples, does not suppress the singular behaviour of the solution. From equation (3.60) we now have

$$f = 2\left\{\frac{(1+\eta)^b(b-\eta) - c(1-\eta)^b(b+\eta)}{(1+\eta)^b + c(1-\eta)^b}\right\},$$

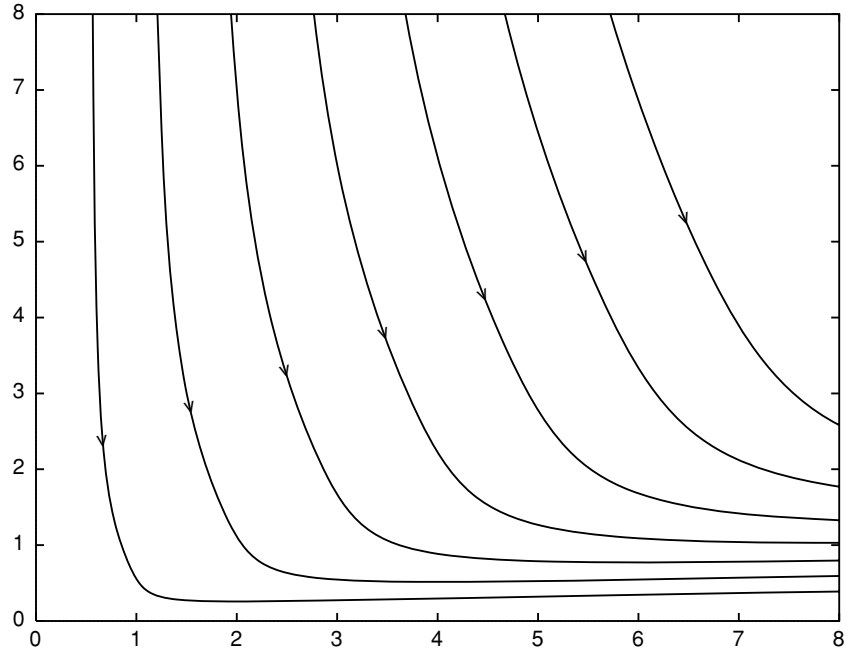

Figure 3.19 As in figure 3.18 except that the flow is bounded by the plane wall $\theta = \frac{1}{2}\pi$. The case shown has $b = 1.88$.

where c is a constant. Berker (1963), making a small correction to Squire's (1955) choice of c, gives

$$c = \left(\frac{1+\eta_0}{1-\eta_0}\right)^b \left(\frac{b-\eta_0}{b+\eta_0}\right),$$

a choice which ensures that $v_\theta = 0$ at $\theta = \theta_0 = \cos^{-1}\eta_0$. It is, therefore, tempting to assume that this solution might represent the flow issuing from the annulus formed by two cones with the same apex and near-identical apex angles. But v_θ is unbounded at the axis $\theta = 0, \pi$, which is, in fact, a line source of strength $m = 4\pi\nu(b-1)$. All the fluid entrained from within this conical, annular jet originates from the line source, which therefore lends a somewhat more artificial air to the solution.

Agrawal (1957) seeks to generalise (3.56) by writing

$$\psi = Kr^n f(\eta)$$

where K is an arbitrary constant. In addition to the solution for $n = 1$, Agrawal recovers the solution for a uniform stream for which $n = 2$, and finds an additional solution for $n = 4$ with

$$f(\eta) = c_1(1-\eta^2) + c_2(1-\eta^2)(1-5\eta^2) + c_3\left\{(1-\eta^2)(3-15\eta^2)\ln\left(\frac{1+\eta}{1-\eta}\right) + 30\eta^3 - 26\eta\right\},$$

where c_1, c_2 and c_3 are arbitrary constants. If singular behaviour at the axis is to be avoided then $c_3 = 0$. A particular example (already encountered in section 3.3) with $c_1 = -c_2 = 1/5$ yields

$$\psi = Kr^4\eta^2(1-\eta^2). \tag{3.62}$$

The flow represented by the stream function (3.62) is a rotational flow, vorticity

$$\boldsymbol{\omega} = 2Kr(1-\eta^2)^{1/2}\hat{\boldsymbol{\phi}},$$

with streamlines that are rectangular hyperbolae, against the plane boundary $\theta = \pi/2$, that is the (x, y)-plane, at which $\mathbf{v} = \mathbf{0}$.

Morgan (1956) has considered solutions of equation (3.60) that represent the flow bounded by either a single cone, or a pair of cones with a common apex. Although the no-slip condition is satisfied at the boundaries, non-trivial solutions are only available when there is transpiration of fluid across them.

3.7.2 The Burgers vortex

The inviscid flow, in a cylindrical polar co-ordinate system,

$$v_r = -kr, \quad v_z = 2kz, \tag{3.63}$$

formed the basis for the earlier study in this chapter of the stagnation flow on a circular cylinder. Suppose the rigid circular cylinder is replaced by a cylindrical vortex core, which induces a circulation Γ at large distances. This suggests a form for the azimuthal velocity as

$$v_\theta = \frac{\Gamma}{2\pi r}g(r), \quad \text{with} \quad g(\infty) = 1. \tag{3.64}$$

Substitution of (3.63), (3.64) into equation (1.20) gives, as the equation for g,

$$r\frac{\mathrm{d}^2 g}{\mathrm{d}r^2} + \left(\frac{r^2 k}{\nu} - 1\right)\frac{\mathrm{d}g}{\mathrm{d}r} = 0,$$

with solution

$$g = 1 - \mathrm{e}^{-\eta}, \quad \text{where} \quad \eta = \frac{kr^2}{2\nu}, \tag{3.65}$$

and the choice $g(0) = 0$ ensures $v_\theta = 0$ at $r = 0$. The vorticity within the core is given by $\boldsymbol{\omega} = (\Gamma/2\pi\nu)\mathrm{e}^{-\eta}\hat{\mathbf{z}}$. This solution discovered by Burgers (see Burgers (1948)), epitomises the dynamics of vorticity discussed in chapter 1, as indeed does the two-dimensional analogue of Robinson and Saffman (1984). The axial velocity v_z stretches the vortex tubes within the core of vorticity and so intensifies it. The vorticity readily diffuses under the action of viscosity, but is restrained by the inward radial convection of vorticity due to the radial velocity v_r.

Sullivan (1959) has extended Burgers' result. If the velocity components are written as

$$v_r = -kr + \frac{1}{r}f(\eta), \quad v_z = 2kz\left\{1 - \frac{f'(\eta)}{2\nu}\right\}, \quad v_\theta = \frac{\Gamma}{2\pi r}\frac{g(\eta)}{g(\infty)}, \tag{3.66}$$

then Sullivan shows that

$$f(\eta) = 6\nu(1 - \mathrm{e}^{-\eta}), \quad g(\eta) = \frac{\nu}{k}\int_0^\eta \exp\left[-t + 3\int_0^t \{(1 - \mathrm{e}^{-s})/s\}\,\mathrm{d}s\right]\mathrm{d}t. \tag{3.67}$$

The structure of the vortical core differs significantly from that of Burgers. For a Burgers vortex $v_r < 0$, $v_\theta > 0$, $v_z/z > 0$ for all r, but from (3.66), (3.67) it can be shown that whilst $v_\theta > 0$ for all r, albeit with a different distribution from (3.64), (3.65), $v_r > 0$ for $\eta \lesssim 2.821$ and $v_z/z < 0$ for $\eta \lesssim 1.099$. As a consequence, whilst the flow assumes the character of a Burgers vortex for $\eta > 2.821$, there is an inner 'cell' within which v_z/z changes sign resulting in a region of counterflow near the axis. The flow therefore assumes, as Sullivan remarks, a two-cell structure.

3.7.3 The influence of boundaries

The Burgers vortex is atypical of real vortices, in the sense that no boundaries are present. Whilst in the solution (3.64), (3.65) k and Γ may be specified independently, the presence of a rigid boundary couples the swirling and, induced, secondary motion.

Long (1958, 1961b), working with cylindrical polar co-ordinates, showed that the Navier–Stokes equations reduce to coupled ordinary differential equations for a conical flow with a line vortex on the half-line $r = 0$, $z \geq 0$. In his solution the circulation Γ about the axis tended to a constant, K, as $r \to \infty$, but the solution did not satisfy $\mathbf{v} = \mathbf{0}$ on the boundary $z = 0$. Whilst the solution is well behaved in the upper half-plane it is singular at $r = z = 0$. As Long observed, his solution can only be expected to be valid at large distances from the bounding surface $z = 0$.

Goldshtik (1960) and Serrin (1972) overcame the difficulty of the bounding surface by developing a solution for which $\mathbf{v} \equiv \mathbf{0}$ on $z = 0$, but at the expense of introducing singular behaviour along the axis. Indeed it appears, as with the round jet discussed above, that for these conical flows it is not possible to have boundaries on which $\mathbf{v} = \mathbf{0}$ without introducing unwanted singular behaviour elsewhere.

As with the round jet it is convenient to use spherical polar co-ordinates, and to supplement (3.56), (3.57) by writing the azimuthal, or swirling, component of velocity and pressure as

$$v_\phi = \frac{C}{r}\frac{\Omega(\eta)}{(1-\eta^2)^{1/2}}, \qquad \frac{p-p_0}{\rho} = \frac{P(\eta)}{r^2(1-\eta^2)} \tag{3.68}$$

where C is related to the circulation. From the radial momentum equation (1.25) the pressure function $P(\eta)$ is given by

$$-2P = f^2 + k^2\Omega^2 + \{ff'' + f'^2 + (1-\eta^2)f''' - 2\eta f''\}(1-\eta^2) \tag{3.69}$$

where $k = C/\nu$ is essentially a Reynolds number. Equations (1.26) and (1.27) then give

$$(1-\eta^2)f^{iv} - 4\eta f''' + ff''' + 3f'f'' = -2k^2\Omega\Omega'/(1-\eta^2), \tag{3.70}$$

and

$$(1-\eta^2)\Omega'' + f\Omega' = 0. \tag{3.71}$$

If the no-slip condition is to be satisfied at the bounding plane $z = 0$, that is $\eta = 0$, then

$$f(0) = f'(0) = \Omega(0) = 0; \tag{3.72}$$

whilst if the vortex, aligned with the axis, is to be neither a line source nor a sink, then

$$f \to 0, \quad \Omega \to 1 \quad \text{as} \quad \eta \to 1, \tag{3.73}$$

corresponding to a line vortex of circulation $\Gamma = 2\pi C$.

Equation (3.70) may be integrated three times to give, with some manipulation and using conditions (3.72)

$$2(1-\eta^2)f' + 4\eta f + f^2 = -2k^2\int_0^\eta \frac{(\eta - t)(1-\eta t)}{(1-t^2)^2}\,\Omega^2\,\mathrm{d}t + k^2(\tilde{P}\eta^2 + \tilde{Q}\eta), \tag{3.74}$$

where the notation of Serrin (1972) has, in part, been retained. Equation (3.74) may be compared with its non-swirling counterpart (3.60). The integral in equation (3.74) converges as $\eta \to 1$. Using (3.73), it may be then inferred that

$(1-\eta)f' \to 0$ as $\eta \to 1$ so that

$$\tilde{P} + \tilde{Q} = 2\int_0^1 \frac{\Omega^2}{(1+t)^2}\mathrm{d}t,$$

and (3.74) may finally be written as

$$2(1-\eta^2)f' + 4\eta f + f^2 = 2k^2(1-\eta)^2\int_0^\eta \frac{t\Omega^2}{(1-t^2)^2}\mathrm{d}t + 2k^2\eta\int_\eta^1 \frac{\Omega^2}{(1+t)^2}\mathrm{d}t + k^2\tilde{P}(\eta^2-\eta). \tag{3.75}$$

The integro-differential system of equations (3.71) and (3.75) has been analysed by Serrin (1972) who also presents numerical solutions for specific pairs $(k, \tilde{P})$ of the two parameters. But there is a difficulty. As $\eta \to 1$ Serrin shows that

$$f \sim \tfrac{1}{8}(\tilde{P}-1)k^2(1-\eta^2)\ln(1-\eta),$$

and this implies

$$v_r \sim -\frac{\nu k^2}{4r}(\tilde{P}-1)\ln(1-\eta) \quad \text{as} \quad \eta \to 1, \tag{3.76}$$

so that not only is the azimuthal velocity component singular, as a line vortex, but so also is the axial component of velocity as $\eta \to 1$. That is, except in the case $\tilde{P} = 1$ which was the case considered by Goldshtik (1960). It has been shown by Goldshtik and Shtern (1990), (see also Goldshtik (1990)), that the singular axial flow (3.76) may be attributed to a line force on $\eta = 1$ given by

$$F_r|_{\eta=1} = \frac{\pi\rho\nu^2}{r}(\tilde{P}-1). \tag{3.77}$$

As Serrin notes there is also an unbalanced radial pressure force, acting towards the axis, close to the bounding surface where the swirling component of velocity reduces to zero. He analyses properties of solutions of (3.71), (3.75) including a delineation of $(k, \tilde{P})$-parameter space where no solutions exist. For the case $\tilde{P} = 1$, considered by Goldshtik (1960) solutions only exist for $k \lesssim 5.53$. Goldshtik and Shtern (1990) analyse the behaviour of solutions as they lose existence, termed 'flow collapse', and also demonstrate non-uniqueness of the solutions considered by Serrin in some parameter sub-region.

The solutions calculated by Serrin are of three distinct types. If $\tilde{P}$ is sufficiently small there is an axial downflow and radial outflow over the bounding plane, whilst if $\tilde{P}$ is sufficiently large, radial inflow is accompanied by axial upflow. For a range of intermediate values of $\tilde{P}$ there is both axial downflow and radial inflow compensated by outflow along a cone $\eta = \eta_0$, say, where $0 < \eta_0 < 1$. These are shown in figure 3.20.

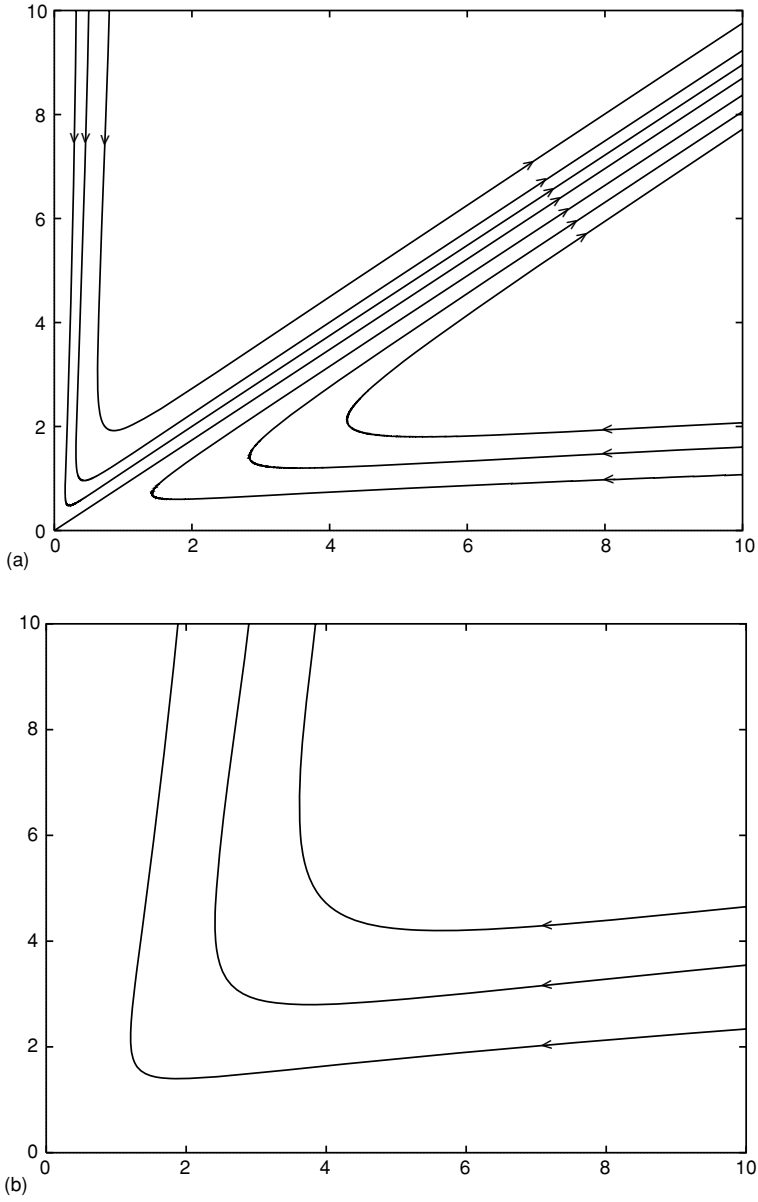

Figure 3.20 Streamline patterns for the bounded vortex configuration of Serrin. (a) $k = 5,\ \tilde{P} = 0.4$. In this case the radial inflow along the boundary and axial downdraught compete, resulting in a funnel-like flow. (b) $k = 3.0,\ \tilde{P} = 1.2$. A case in which the downdraught is overwhelmed by the radial inflow. (c) $k = 3.5$, $\tilde{P} = 0.2$. The obverse of (ii).

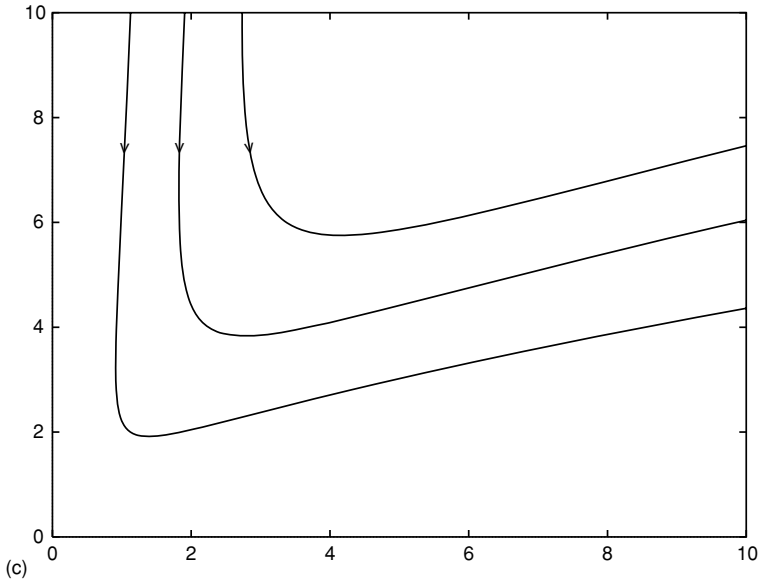

Figure 3.20 (*cont.*)

In figure 3.21 we show radial velocity profiles correponding to the three types of solution shown in figure 3.20.

Whilst refraining from a claim that his solutions represent physical phenomena, there are clearly features reflecting the behaviour of tornadoes and waterspouts; Serrin draws attention to Morton (1966) for an account both of the relation of the concentrated vortex core to the main motion and of the driving mechanisms likely to be involved in typical tornado and waterspout phenomena.

Yih, Wu, Garg and Leibovich (1982) also consider a conical vortex flow of the type represented by equations (3.56) to (3.58) and (3.68), governed by the differential equations (3.70) and (3.71). The flow is bounded by the cone $\theta = \theta_0$, with the special case $\theta_0 = \pi/2$ corresponding to that of Goldshtik (1960) and Serrin (1972). However, unlike Goldshtik and Serrin, they relax the no-slip condition at the solid boundary but insist that velocities be finite along the axis. In that case the boundary conditions require

$$f(\eta_0) = 0, \quad \Omega(\eta_0) = 1, \quad f(1) = \Omega(1) = 0, \quad \lim_{\eta \to 1}(1 - \eta^2) f''(\eta) = 0,$$

where, with C arbitrary in (3.68), the condition on Ω at the boundary establishes the level of swirl. The solution is not entirely free from singularities; there is a singularity at the cone vertex which Yih *et al.* interpret as a source of axial

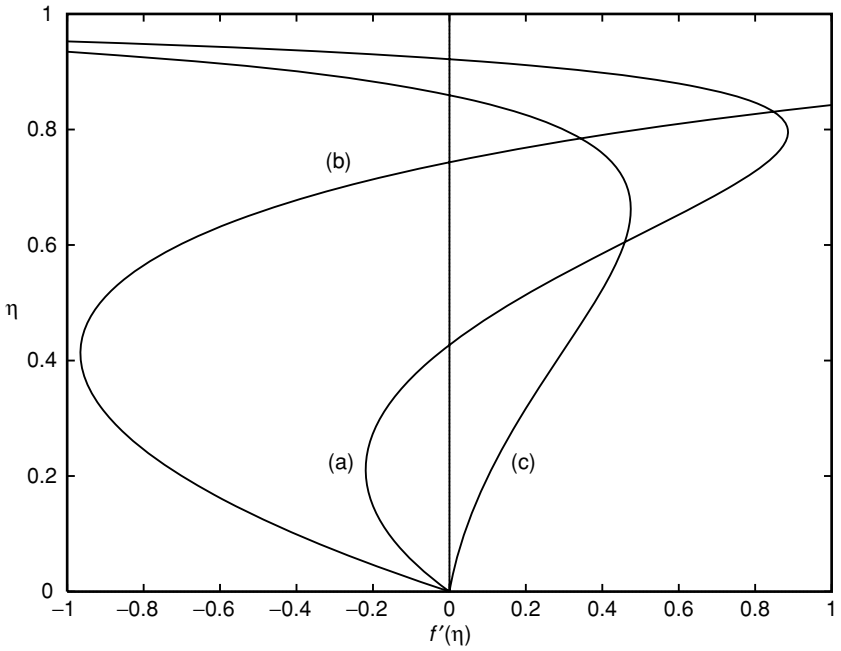

Figure 3.21 Radial velocity profiles $rv_r/\nu = f'(\eta)$ corresponding to the streamline patterns of figures 3.20 (a), (b), (c).

momentum. Numerical solutions are presented for cases $\theta_0 = \pi/4, \pi/2, 3\pi/4$. For the case of a plane boundary, $\theta = \pi/2$, solutions similar to each of the three types shown in figure 3.20 are shown. In a subsequent paper Sozou (1992) extends the work of Yih *et al.* by introducing a source of vorticity at the vertex of the cone. Formal existence of the class of solutions obtained by Yih *et al.* has been established by Stein (2000). Stein (2001) has also addressed the problem of uniqueness, showing that the solutions are unique for $\theta_0 \leq \pi/2$, but not for $\theta_0 > \pi/2$ where in at least one case non-uniquness has been demonstrated.

In a series of papers Pillow and Paull (1985), Paull and Pillow (1985a, 1985b) carry out a comprehensive investigation of conically similar viscous flows. In particular they seek types of axial causes of such flows. For flows of the type studied by Serrin (1972) they identify the force (3.77), whilst for those of Yih *et al.* (1982) semi-infinite line sources of angular momentum generate such swirling flows.